Corrosion protection

Jacek Banaś

University of Science and Technology (AGH-UST)
Faculty of Foundry Engineering
Department of General and Analytical Chemistry

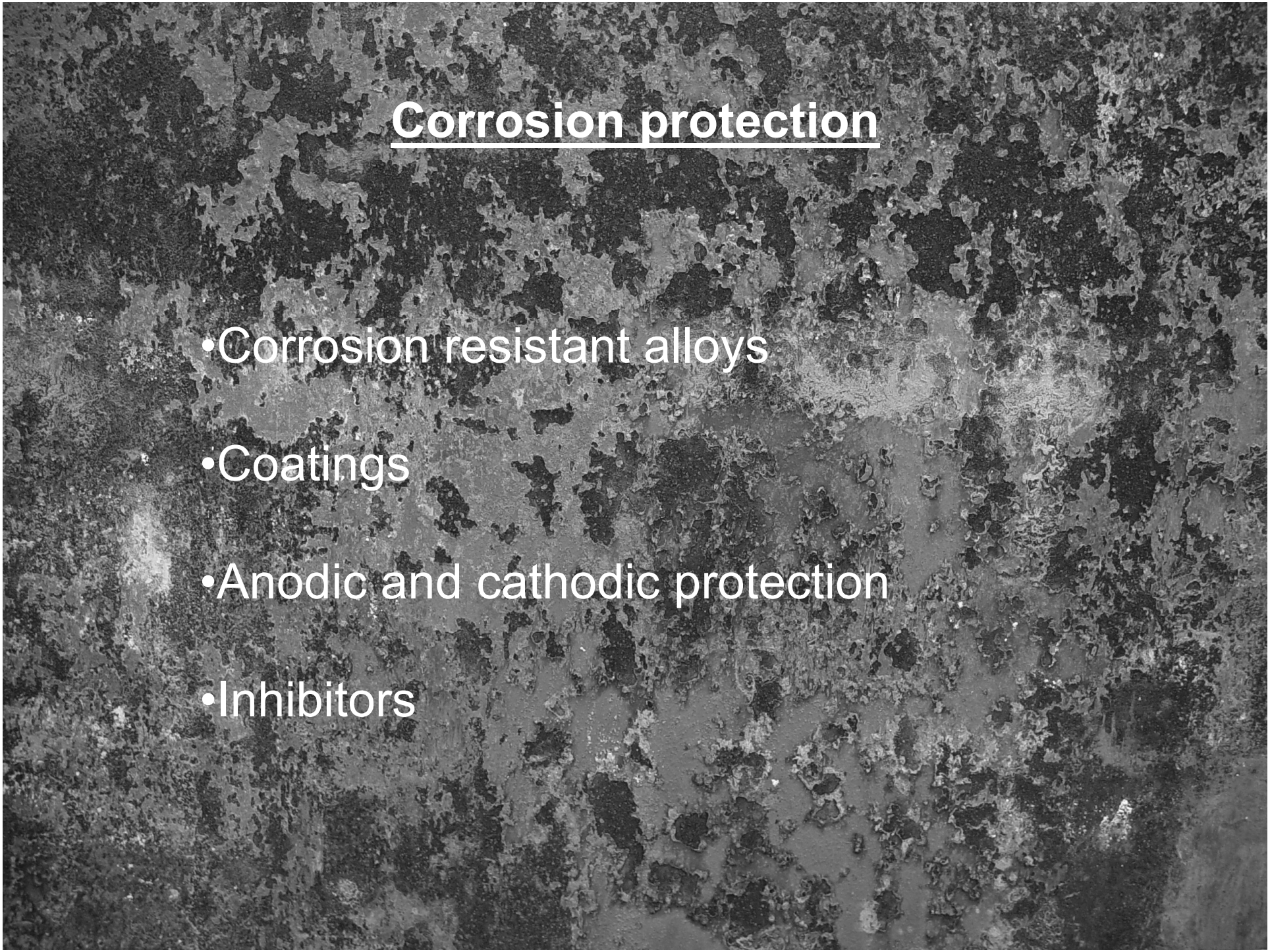
Corrosion protection
•Corrosion resistant alloys
•Coatings
•Anodic and cathodic protection
•Inhibitors

CORROSION RESISTANT ALLOYS

active, passive and transpassive state

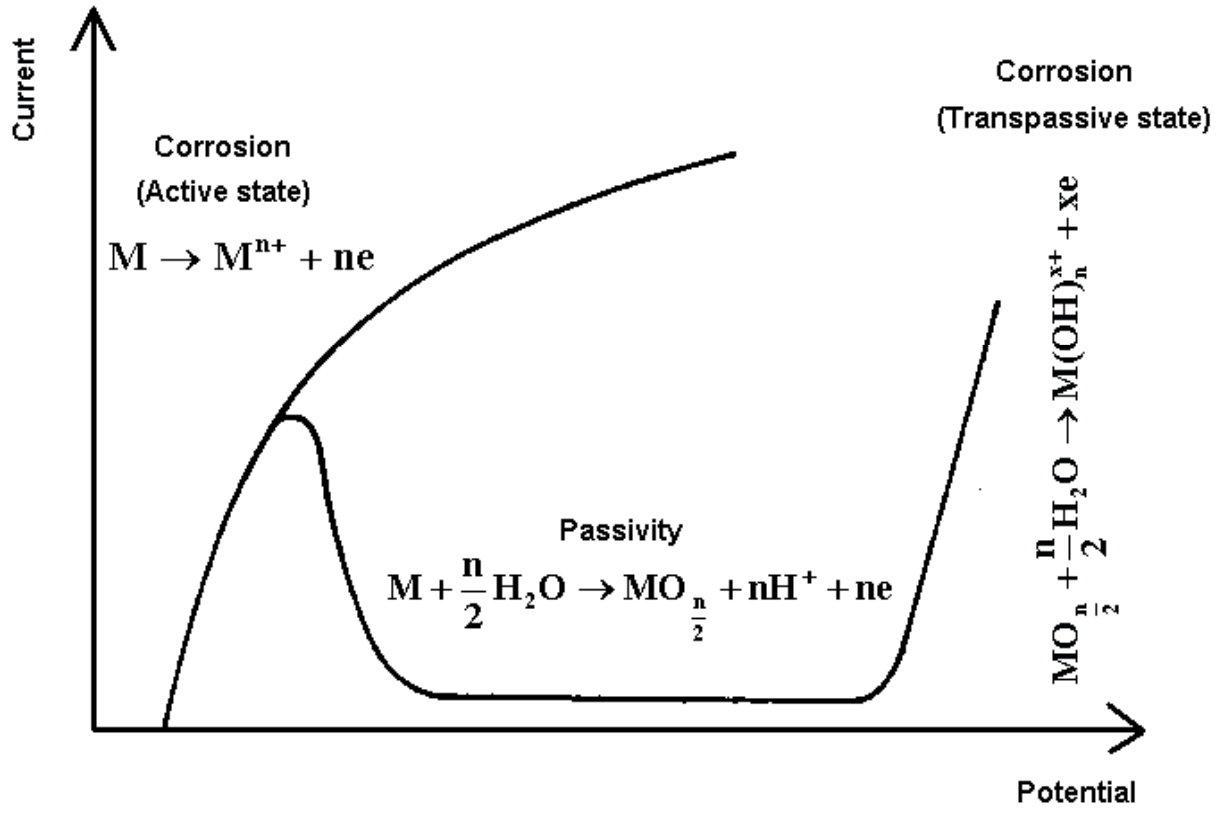

Anodic polarization curves of metal undergoing corrosion and passivation

Iron alloys

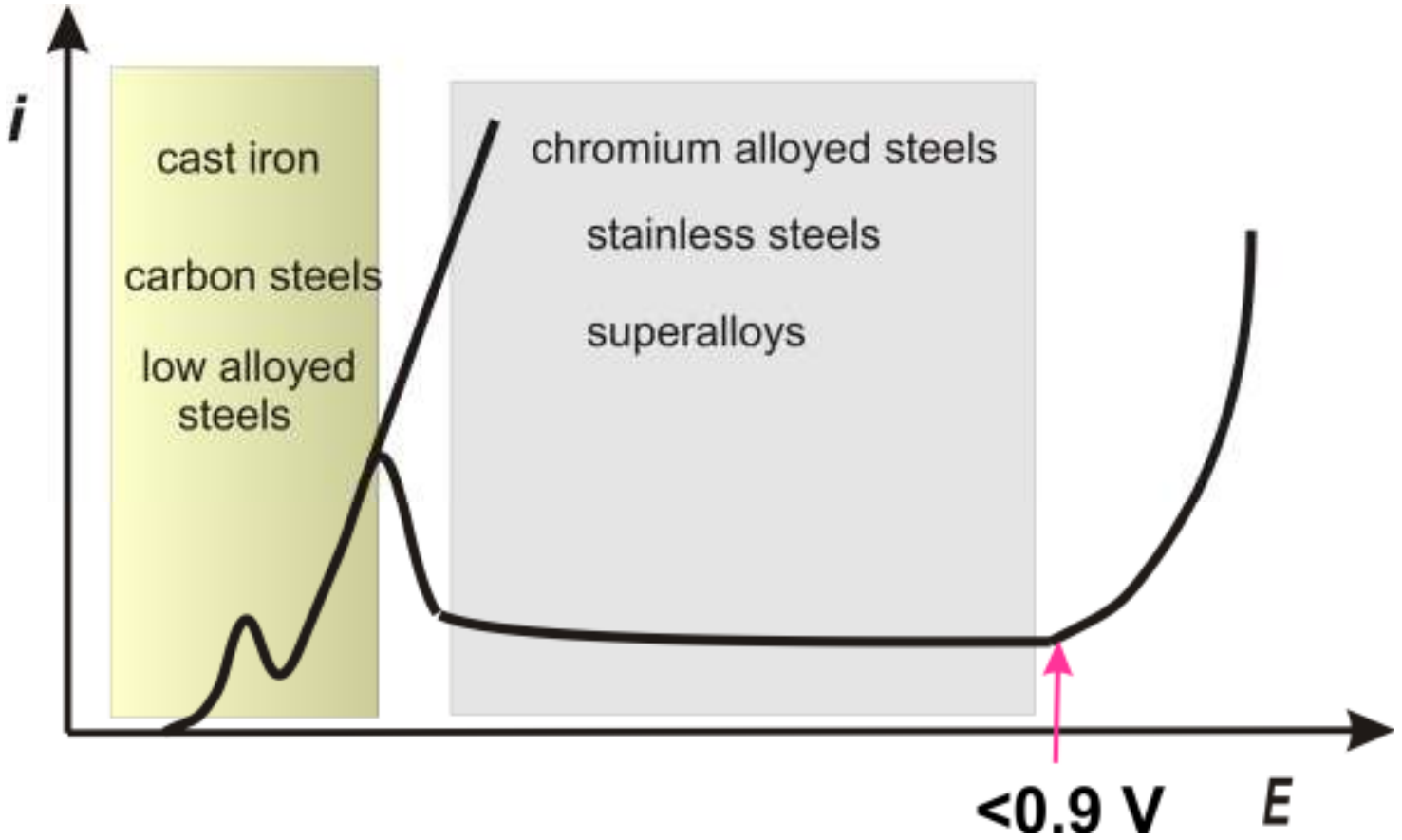

> 13 -14 %Cr

≥ 18 %Cr stainless steels

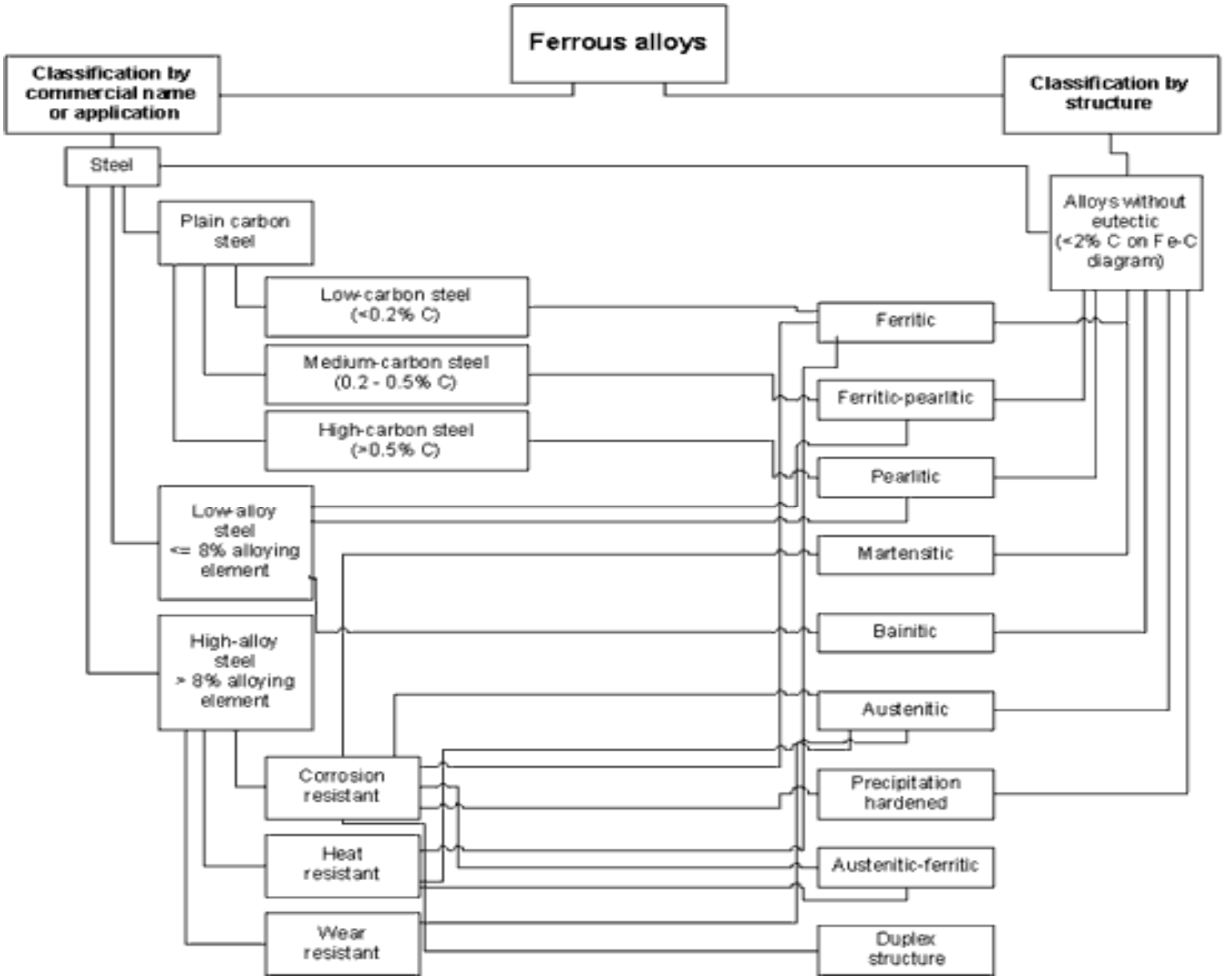
Ferrous alloys
Classification by commercial name or application
Classification by structure
Steel
Plain carbon steel
Low-carbon steel (<0.2% C)
Medium-carbon steel (0.2 - 0.5% C)
High-carbon steel (>0.5% C)
Low-alloy steel <= 8% alloying element
High-alloy steel > 8% alloying element
Corrosion resistant
Heat resistant
Wear resistant
Alloys without eutectic (<2% C on Fe-C diagram)
Ferritic
Ferritic-pearlitic
Pearlitic
Martensitic
Bainitic
Austenitic
Precipitation hardened
Austenitic-ferritic
Duplex structure

Steels can be classified by a variety of different systems depending on:

- The composition, such as carbon, low-alloy or stainless steel.
- The finishing method, such as hot rolling or cold rolling
- The product form, such as bar plate, sheet, strip, tubing or structural shape
- The deoxidation practice, such as killed, semi-killed, capped or rimmed steel
- The microstructure, such as ferritic, pearlitic and martensitic
- The required strength level, as specified in ASTM standards
- The heat treatment, such as annealing, quenching and tempering, and thermomechanical processing
- The manufacturing methods, such as open hearth, basic oxygen process, or electric furnace methods.
- Quality descriptors, such as forging quality and commercial quality.

Low-alloy steels can be classified according to:

•*Chemical composition*, such as nickel steels, nickel-chromium steels, molybdenum steels, chromium-molybdenum steels

•*Heat treatment*, such as quenched and tempered, normalized and tempered,

Low-carbon quenched and tempered steels combine high yield strength (from 350 to 1035 MPa) and high tensile strength with good notch toughness, ductility, corrosion resistance, or weldability.
Medium-carbon ultrahigh-strength steels are structural steels with yield strengths that can exceed 1380 MPa.
Bearing steels used for ball and roller bearing applications are comprised of low carbon (0.10 to 0.20% **C**) case-hardened steels and high carbon (-1.0% C) through-hardened steels. Many of these steels are covered by SAE/AISI designations.
Chromium-molybdenum heat-resistant steels contain 0.5 to 9% **Cr** and 0.5 to 1.0% **Mo**. The carbon content is usually below 0.2%. The chromium provides improved oxidation and corrosion resistance, and the molybdenum increases strength at elevated temperatures. They are generally supplied in the normalized and tempered, quenched and tempered or annealed condition. Chromium-molybdenum steels are widely used in the oil and gas industries and in fossil fuel and nuclear power plants.

CORROSION RESISTANT ALLOYS

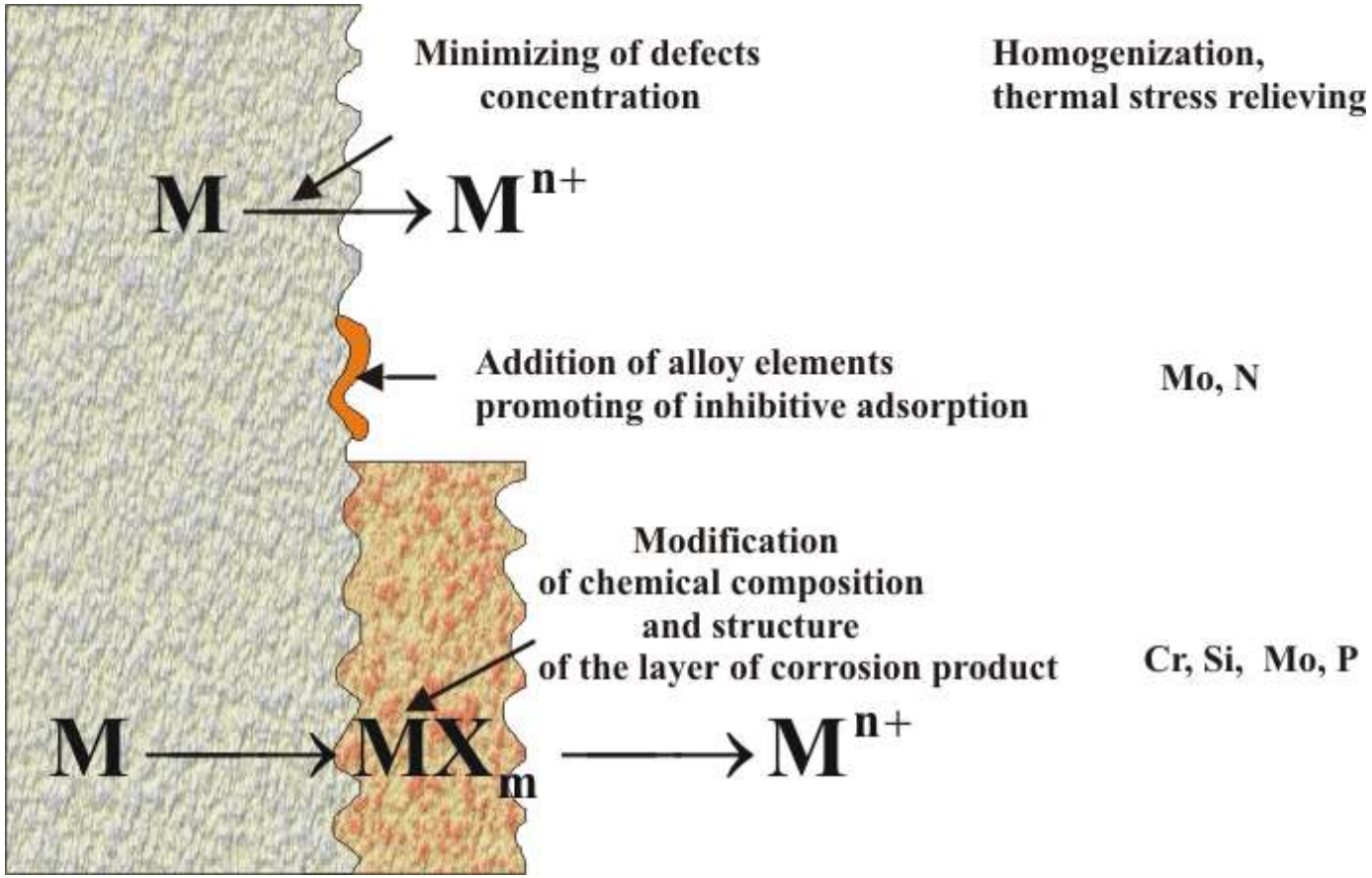

Schematic presentation of the factors improving corrosion resistance of active alloys

Chemical composition of corrosion products on iron in water saturated by air

Fe II compounds

$Fe(OH)_2$, $FeCO_3$ (syderyt)

Fe III compounds

$5Fe_2O_3 \cdot 9H_2O$, $Fe(OH)_3$, α FeOOH (getyt), γFeOOH (lepidocrocyte) ,

Fe II + FeIII compounds

Fe_3O_4 , ($Fe_4^{II}Fe_2^{III}(OH)_{12}CO_3$) (green rust, FeII / FeIII ration changes in the interval from4 to 0.8)

Calcium carbonate deposit

$CaCO_3$

M.M. Benjamin i inni: „ Internal corrosion of water distribution systems" Cooperative Research Report AWWA Denver Co, 1996

Alloying by addition of the inhibiting components and components improving protective behavior of surface layer

Some non metallic **(P,N, Si)** and metallic **(Cr, Mo)** components of the alloy can accumulate on active places of metal surface during corrosion process. These elements react with the solvent and form non soluble strongly adsorbed compounds on the kinks, steps and structural defects. The blocking of active areas of the alloy surface leads to the decrease of corrosion rate.

The adsorbed intermediate product can influence kinetics of growth of the layer of corrosion product and can change their microstructure and morphology. The reason of the better corrosion resistance of weathering steels in atmosphere in compare to ordinary carbon steels is the presence of small amounts of **Cr, Mo, Si, P**. The above mentioned elements change the microstructure of iron oxides on the steel surface

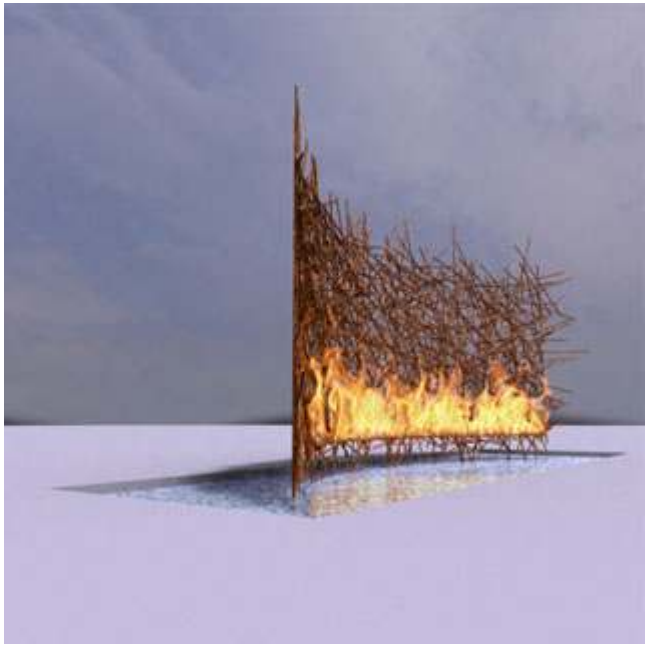

The protective properties of the films formed on **weathering steels** are connected with the presence of **superparamagnetic goethite and maghemite** in the inner layer. The decrease of particle size of goethite and maghemite increases protective behavior of the surface layer. The presence of silicon and phosphorus in the weathering steels stimulates the formation of superparamagnetic goethite and thus improves the corrosion resistance of the alloys


weathering steels

Optimal composition of carbon steel resistant to hydrogen embrittlement

Component	Optimal content %
C	0.2 do 0.3
Solid state components Si Mn Ni Co Al	0.4 do 0.7 ≤ 1.2 0.5 do 1.0 ≤ 0.5 ≤ 0.25
Carbides formers Cr Mo Ti Nb V	1.0 do 1.5 0.4 do 0.5 0.05 0.02 do 0.06 0.1
Modifiers REM (Ce) AlN, VN, NbN	0.1 do 0.3 0.2
Impurities S P Sb Sn Cu	≤ 0.01 ≤ 0.015 ≤ 0.01 ≤ 0.01 ≤ 0.05

Corrosion of cast iron

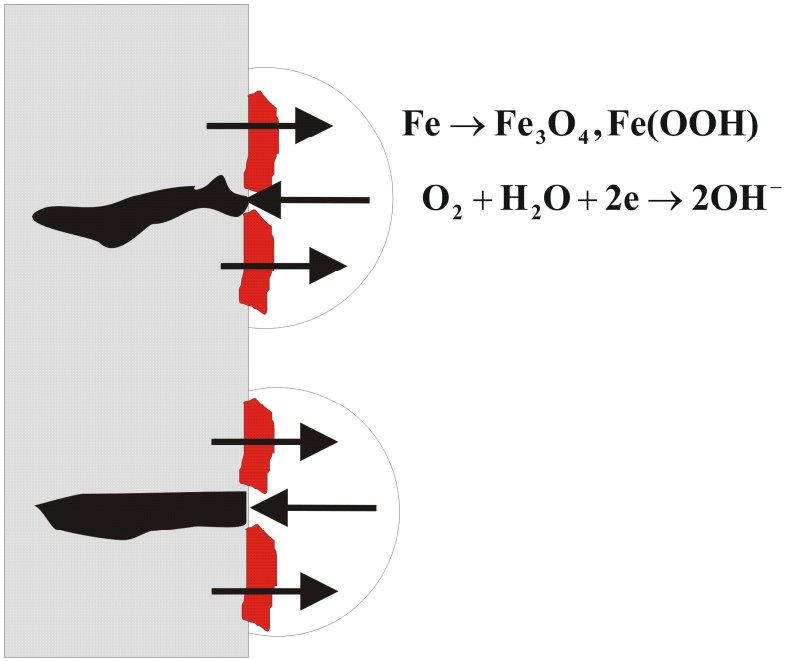

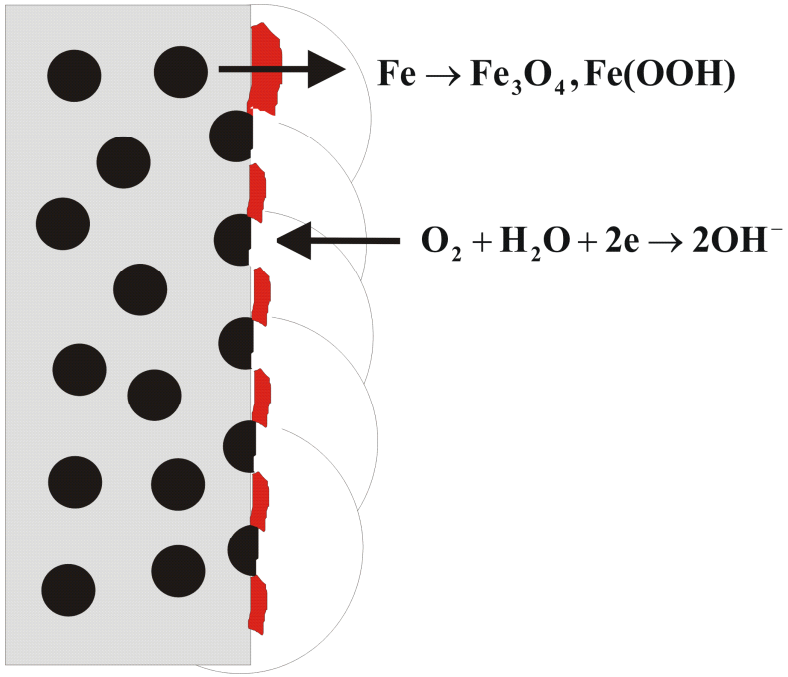

Grey cast iron

Ductile cast iron

Graphite– ferrite galvanic elements in cast iron

Corrosion of cast iron

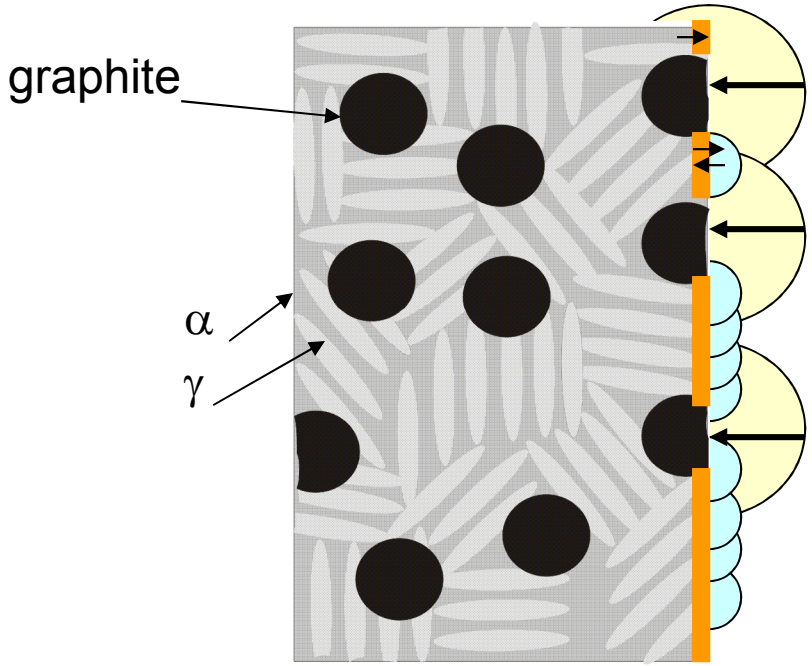

Galvanic elements in ausferrite cast iron

Corrosion rate of cast iron and carbon steel in atmosphere

Alloy	Corrosion rate, g / cm^2 d		
	Rural atmosphere	Industrial atmosphere	Marine atmosphere
Carbon steel	1.0	1.6 – 3.4	2.7 – 3.6
Grey cast iron		1.1 - 3.2	0.6
Perlitic ductile cast iron	0.6	1.3	0.9 – 1.0
Ferritic ductile cast iron	0.9	1.2	1.6

Passive metals

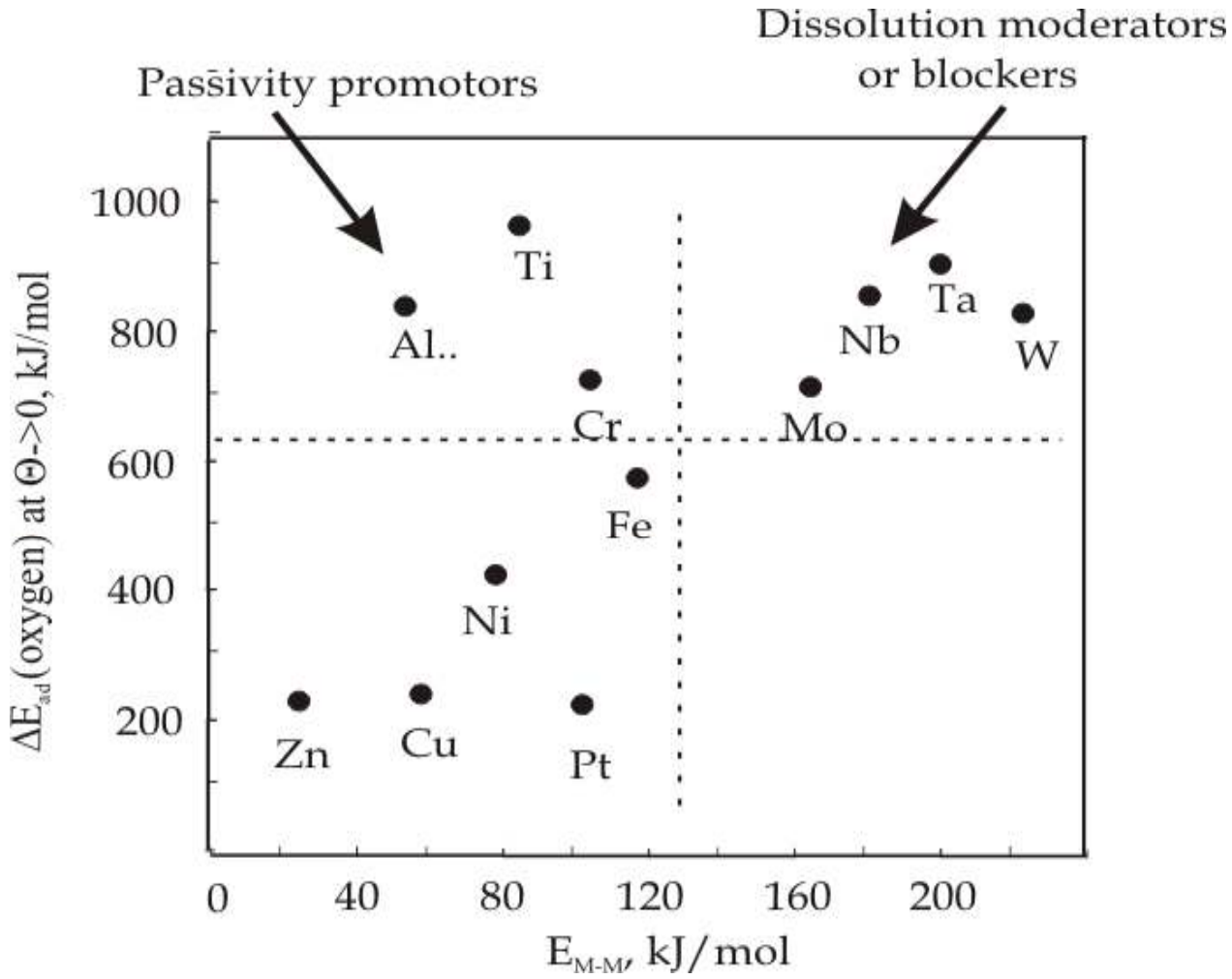

Passivity promoters and dissolution moderators according to the synergy between the energy of the metal-metal bonds and heat of adsorption of oxygen.

P. Marcus: Corr.Sci. 36, 2155 (1994)

Polarisation behaviour of stainless steels

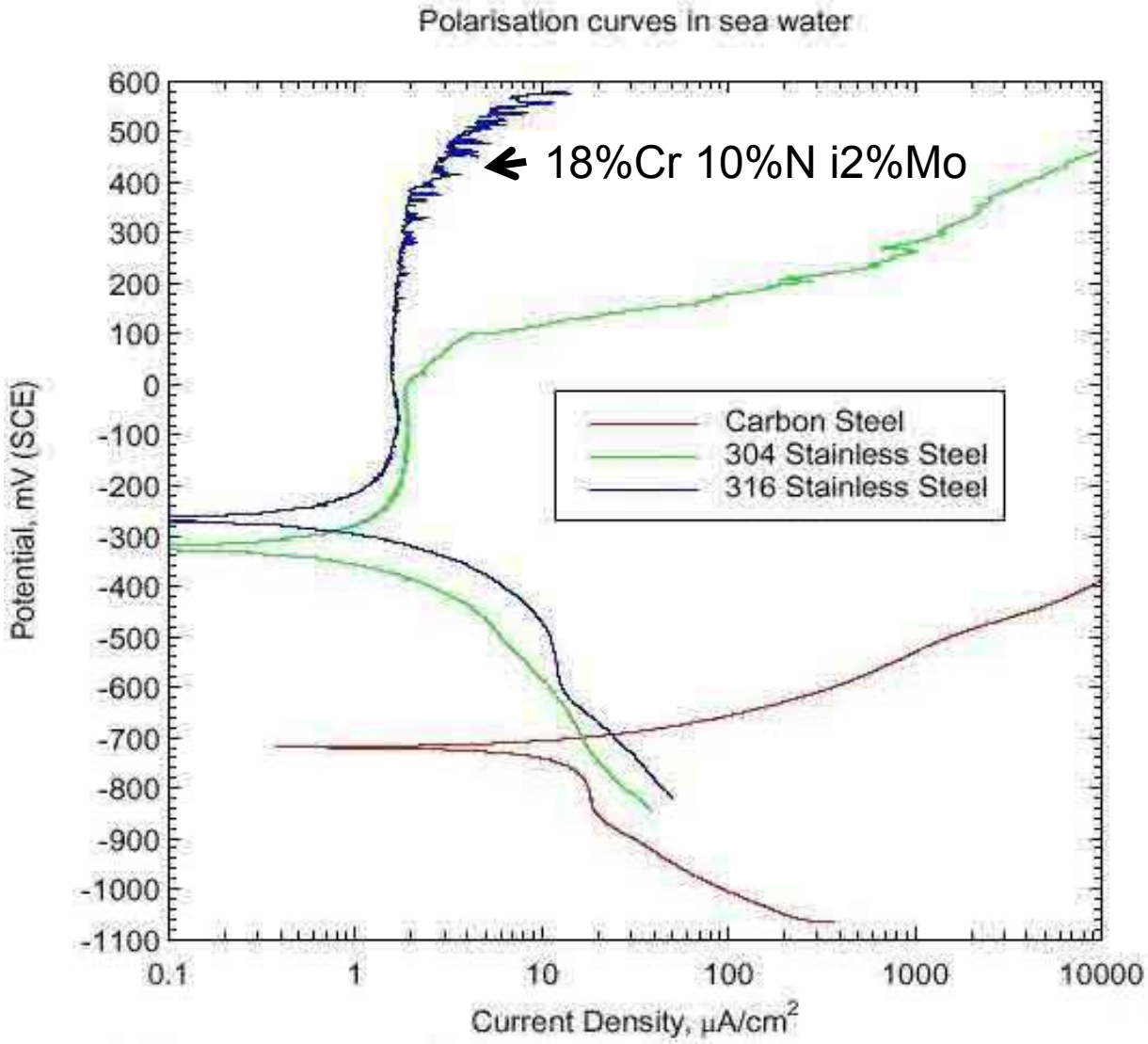

Corrosion behaviour of stainless steels

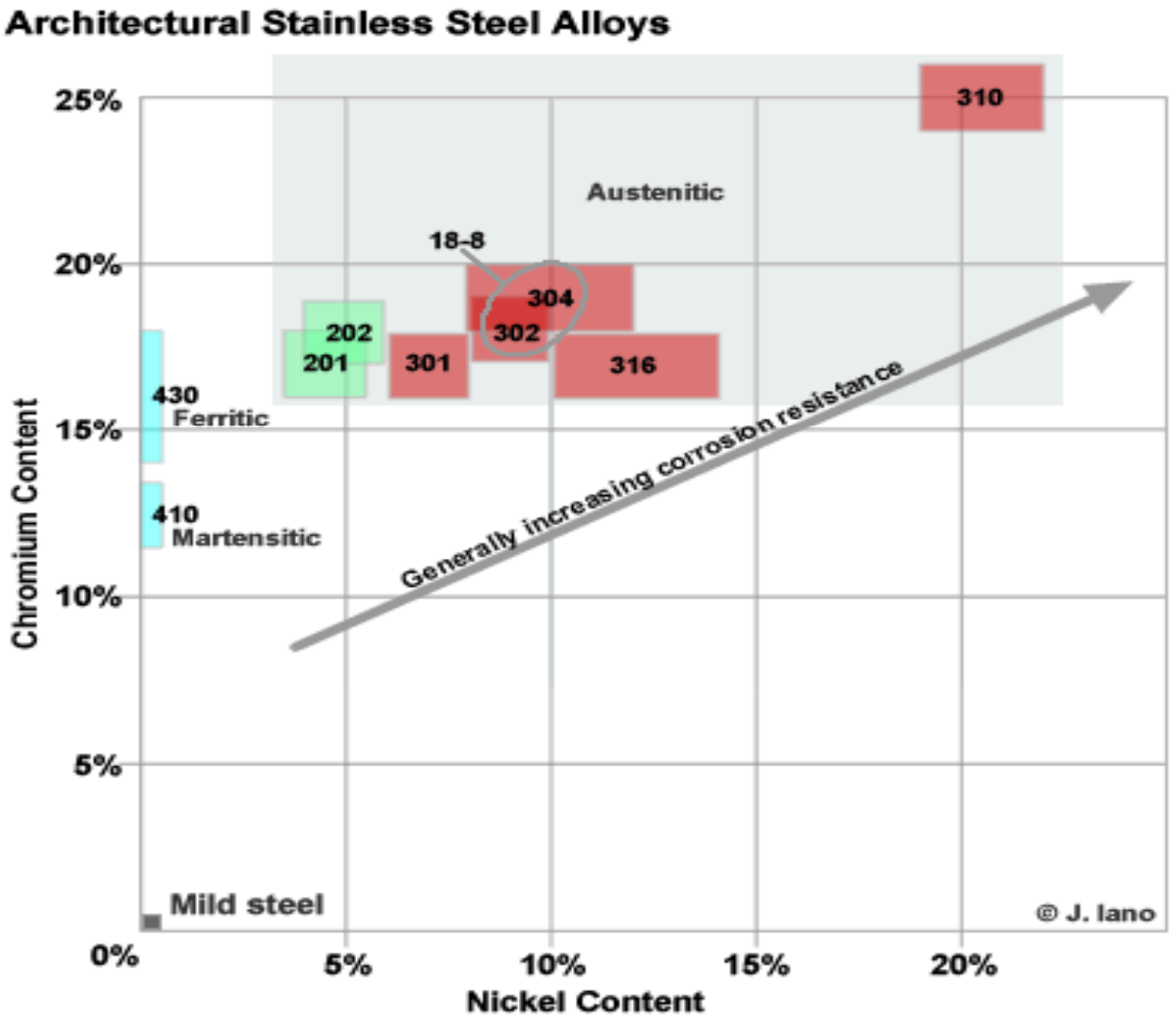

Environmental and metallurgical limits for some stainless steels when used for any type of equipment or component according to NACE MR0175/ISO 15156-3:2003

Materials	Max. temp. (°C)	Max. p_{H_2S} (kPa)	Max. Cl^- conc. (mg/l)	pH	Remarks
Ferritic stainless steels	[1]	10	[1]	≥3.5	Shall be in the annealed condition and shall have maximum hardness of 22 HRC.
Martensitic stainless steels	[1]	10	[1]	≥3.5	See standard for heat-treatment. Shall have a maximum hardness of 22 HRC.
Austenitic stainless steels	60 [3]	100 [3]	[2] 50	[2] [3]	Shall be in the solution-annealed and quenched condition, be free of cold work intended to enhance their mechanical properties and have a maximum hardness of 22 HRC.
Highly alloyed austenitic stainless steels (Ni+2Mo) > 30, Mo ≥ 2	60 [3]	100 50	[2] [3]	[2] [3]	Shall be in the solution-annealed conditions
Highly alloyed austenitic stainless steels PREN >40	60 [3] 121 149 171	100 50 700 310 100	[2] [3] 5 000 5 000 5 000	[2] [3] [4] [4] [4]	Shall be in the solution-annealed conditions.
Duplex stainless steels 30 ≤ PREN ≤ 40, Mo ≥ 1.5	232	10	[2]	[2]	Shall be solution annealed and liquid-quenched, have a ferrite content of between 35 and 65% and not have undergone ageing heat-treatments.
Duplex stainless steels 40 ≤ PREN ≤ 45	232	20	[2]	[2]	

Corrosion behaviour of stainless steels

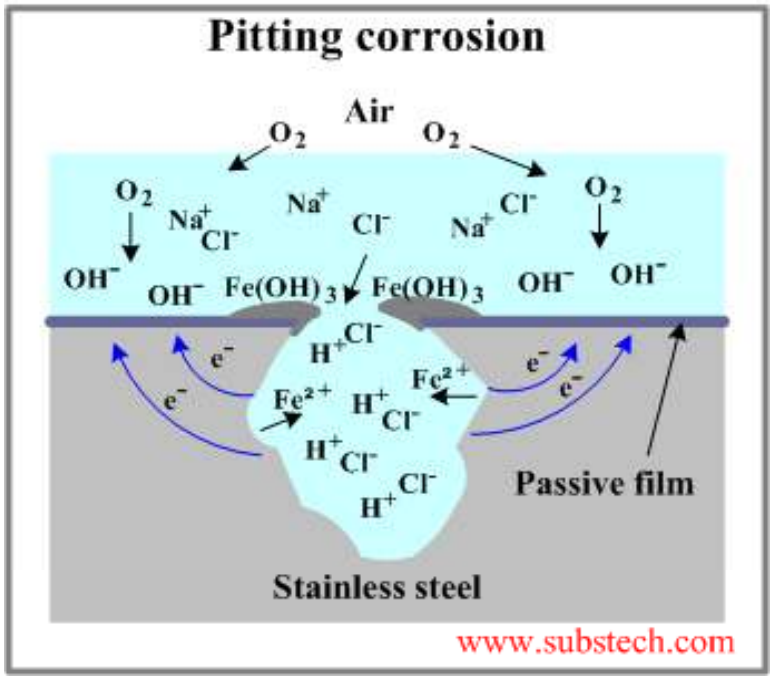

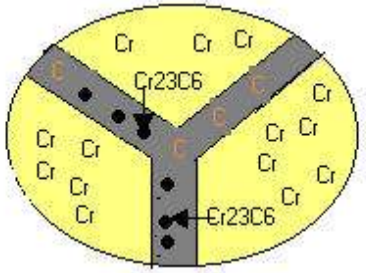

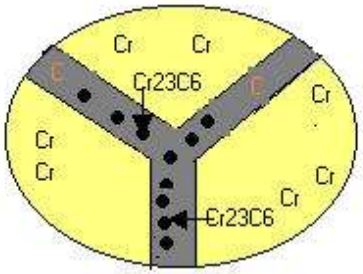

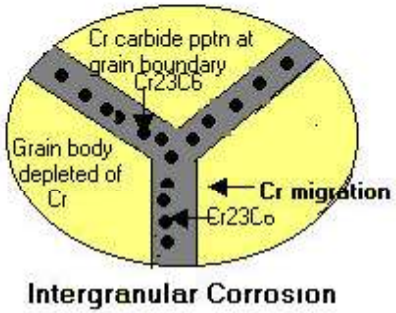

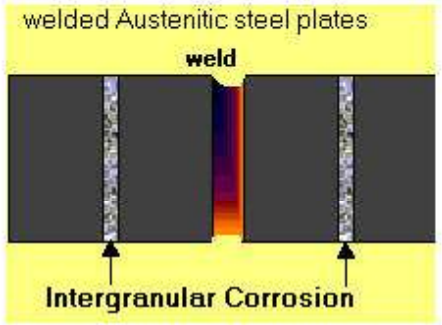

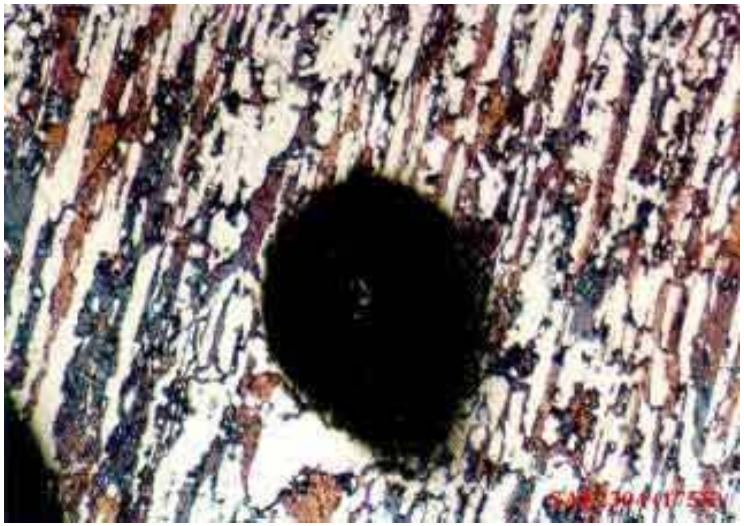

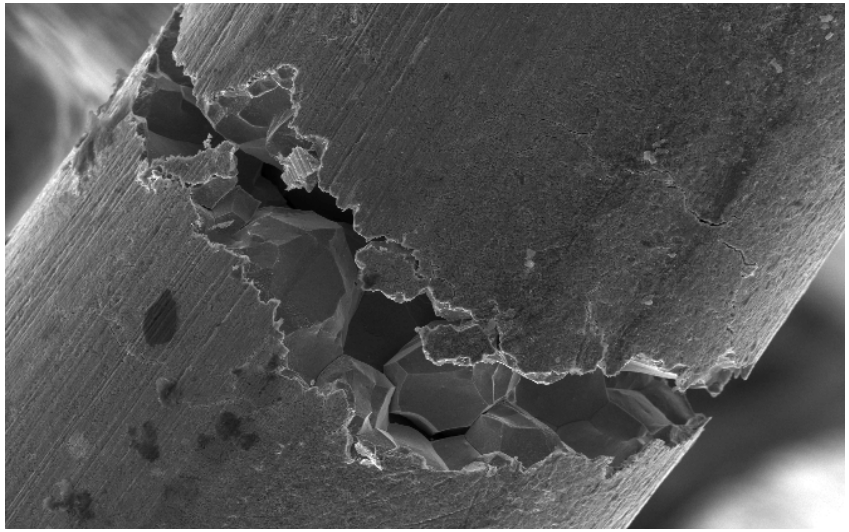

Typical composition and PREN values for some stainless steel grades

PREN = %Cr + 3.3 x (%Mo + 0.5 x %W) + 16 x %N.

Steel grade	Typical composition, % by weight					PREN[1]
	Cr	Ni	Mo	N	Others	
Austenitic						
4404	17.2	10.1	2.1	-	-	24
904L	20	25	4.3	-	1.5Cu	34
254 SMO®	20	18	6.1	0.20	Cu	43
4565	24	17	4.5	0.45	5.5Mn	46
654 SMO®	24	22	7.3	0.50	Mn, Cu	56
Duplex						
LDX 2101®	21.5	1.5	0.3	0.22	5Mn	26
2304	23	4.8	0.3	0.10	-	26
2205	22	5.7	3.1	0.17	-	35
2507	25	7	4	0.27	-	43

Passivity of stainless steels in thermal water

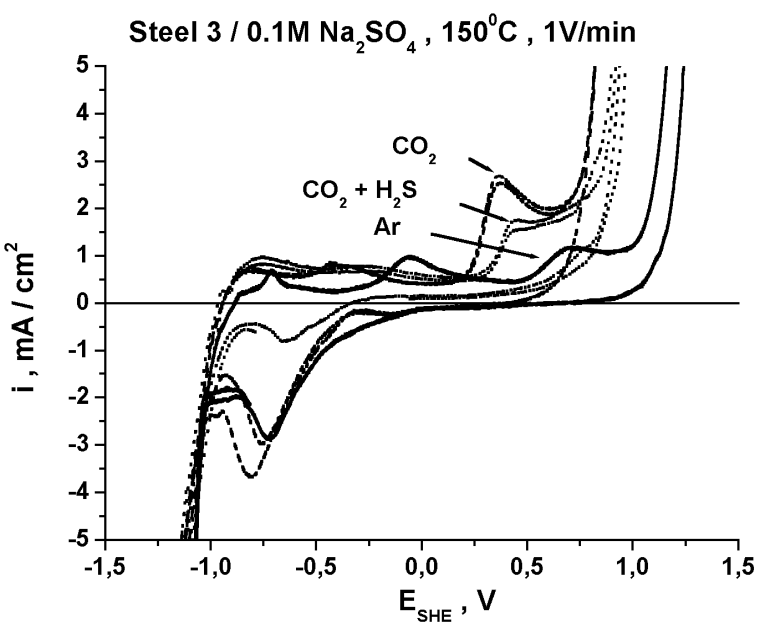

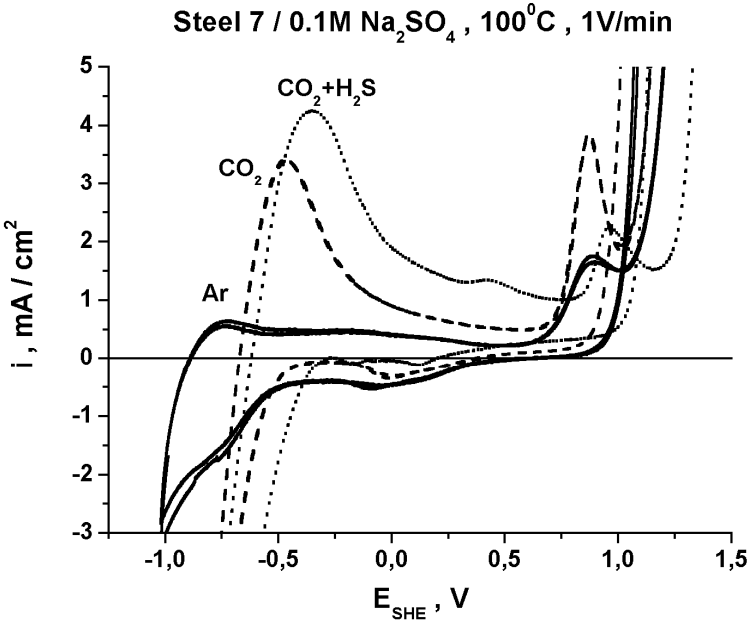

LSV curves of ferritic alloy Fe-22%Cr (a) and austenitic alloy Fe-22%Cr-25%Ni (b) in 0.1M Na_2SO_4 saturated with Ar, CO_2 and CO_2 + 1%H_2S, at 150^{0}C


Copper Alloys

Copper Alloys

Manganese Bronze and Architectural Bronze

Aluminium Bronze

Silicon Bronze

Phosphor bronzes, tin bronzes

CuZn40Mn1Pb1 (CW720R) brass

CuZn41Pb1Al brass

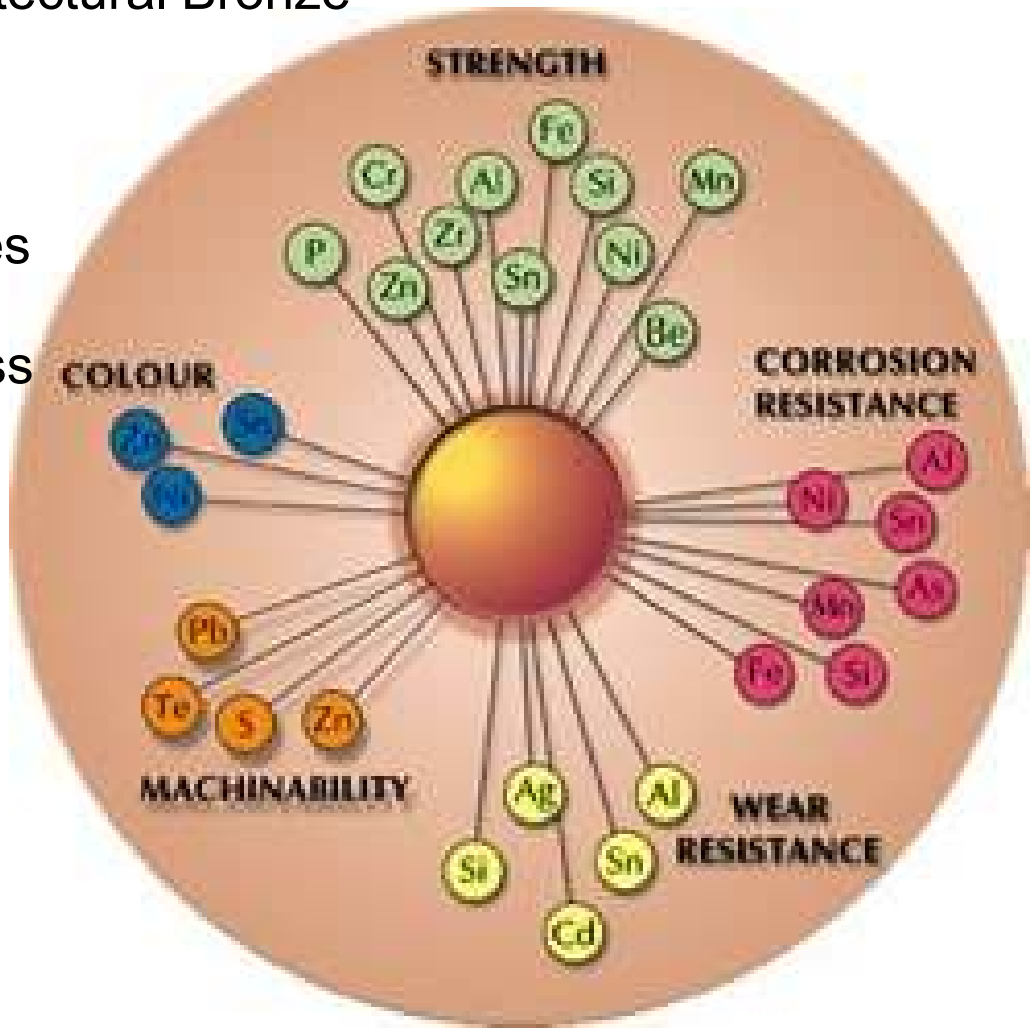

Copper-nickel

Applications

- Sea water pipework
- Offshore fire water systems
- Heat exchangers and condensers
- Sheathing of legs and risers on offshore platforms and boat hulls
- Hydraulic lines
- Fish cages for aquaculture
- Desalination units.

Corrosion of copper alloys

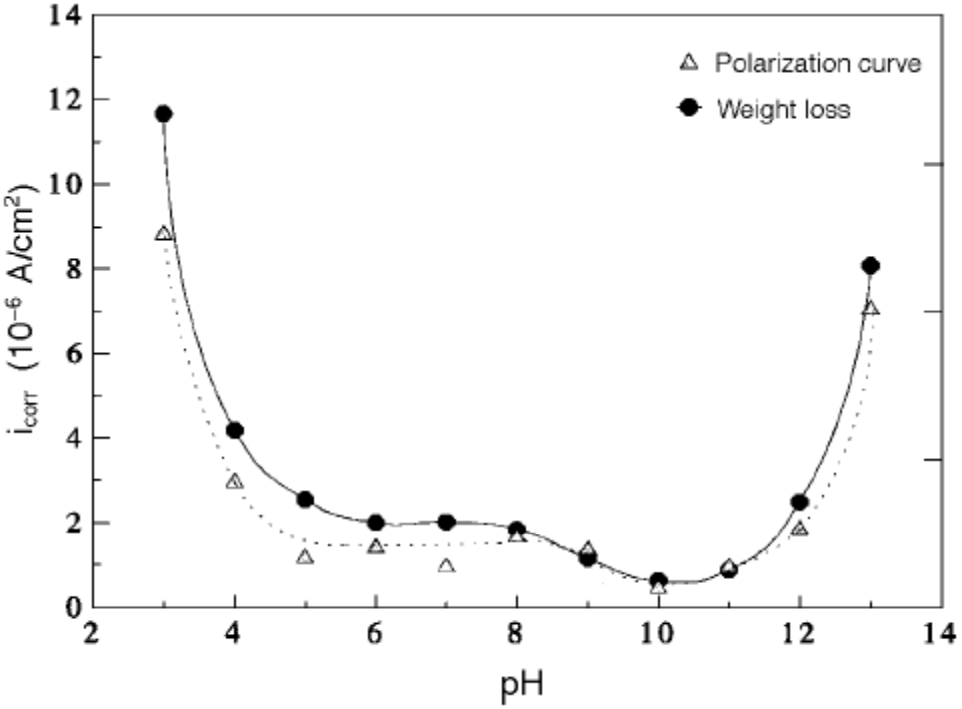

icorr of copper in the solutions
of various pH values
(T = 30°C, immersion time 24 h).

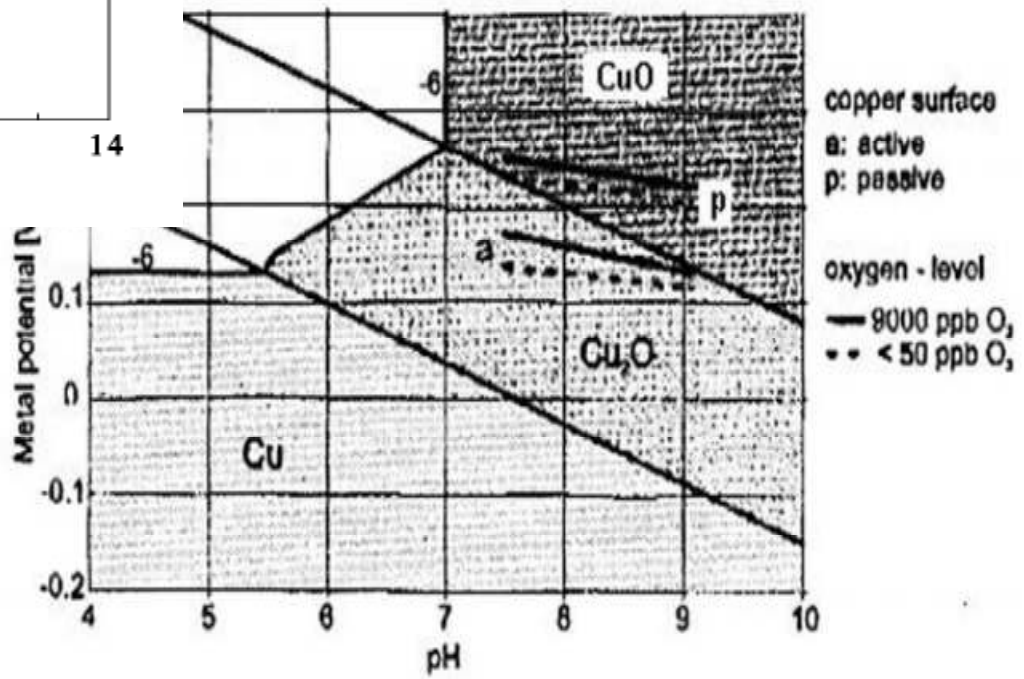

Corrosion of copper alloys

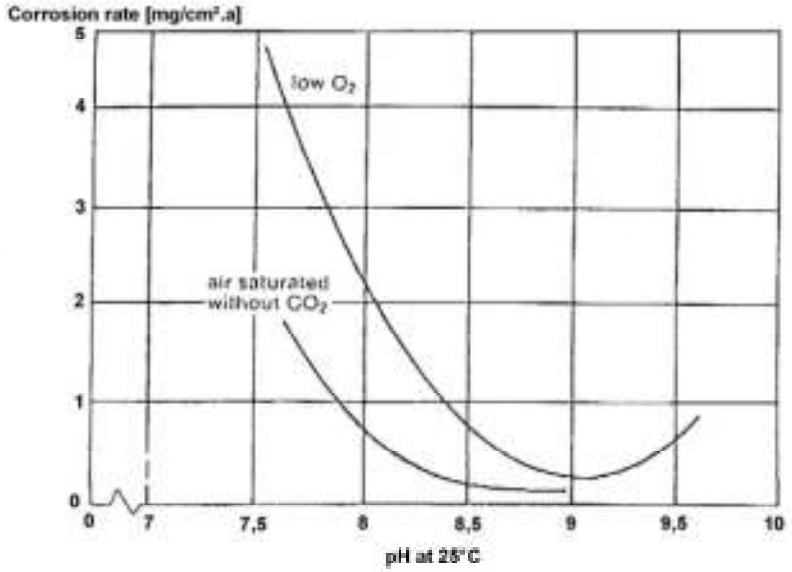

Corrosion of copper in tap water

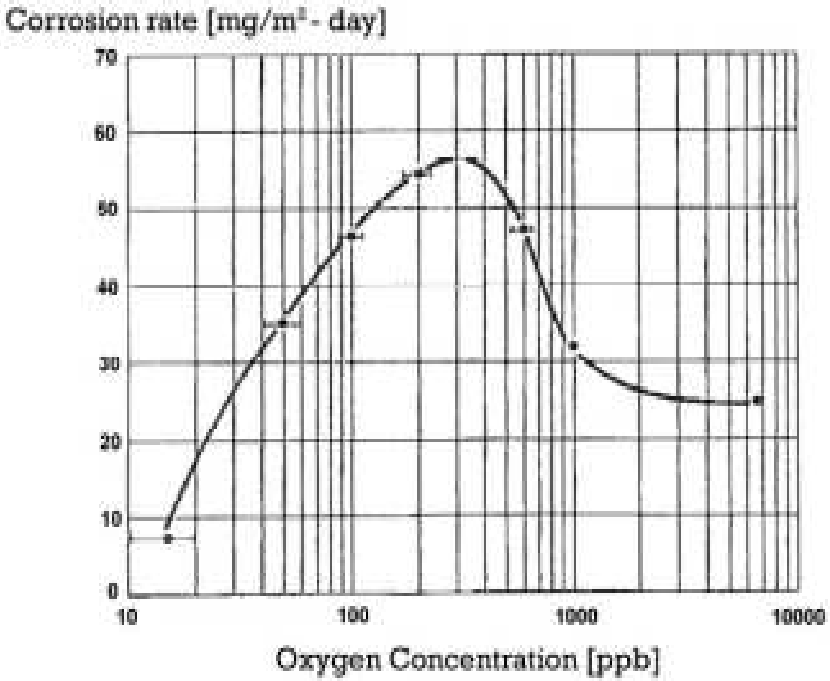

CORROSION STABILITY OF DIFFERENT BRONZES IN SIMULATED URBAN RAIN

Erika Švara Fabjan, Tadeja Kosec, Viljem Kuhar, Andraž Legat

ISSN 1580-2949
MTAEC9, 45(6)585(2011)

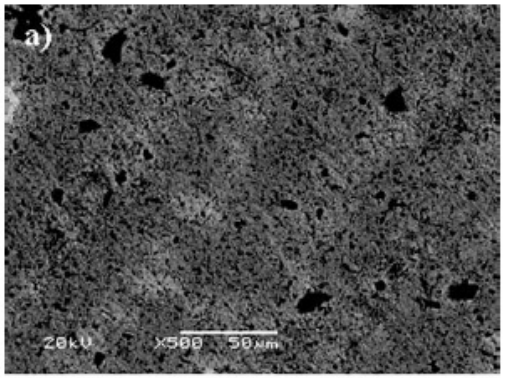

Brohanite $Cu_4SO_4(OH)_6$

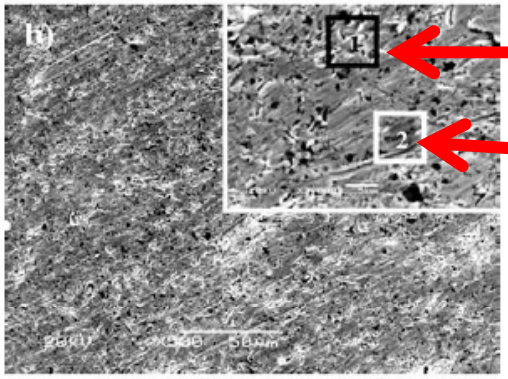

$CuCO_3$

Cu_2O and SnO_2

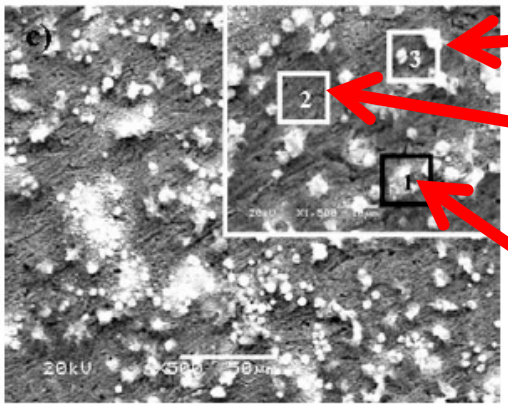

Brohanite $Cu_4SO_4(OH)_6$
< naukarite $Cu_4SO_4(CO_3)(OH)_6 48H_2O$

SiO_2 and SnO_2

Brohanite $Cu_4SO_4(OH)_6$
or naukarite $Cu_4SO_4(CO_3)(OH)_6 48H_2O$

	Bronze alloy / Composition	Cu	Sn	Zn	Pb	Si	Al	P	Fe	the rest
a	CuSnZn	87.0	5.5	3.6	0.1	–	0.6	–	0.1	3.1
b	CuSnZnPb	87.1	6.6	1.1	5.0	–	–	0.1	0.1	0
c	CuSnSi	85.5	9.6	0.1	0.1	2.5	–	0.1	0.1	2.0

DEZINCIFICATION OF BRASS

Dezincification is an example of "dealloying" in which one of the constituents of an alloy is preferentially removed by corrosion.

Dezincification can be caused by water containing sulfur, carbon dioxide and oxygen. Stagnant or low velocity waters tend to promote dezincification.

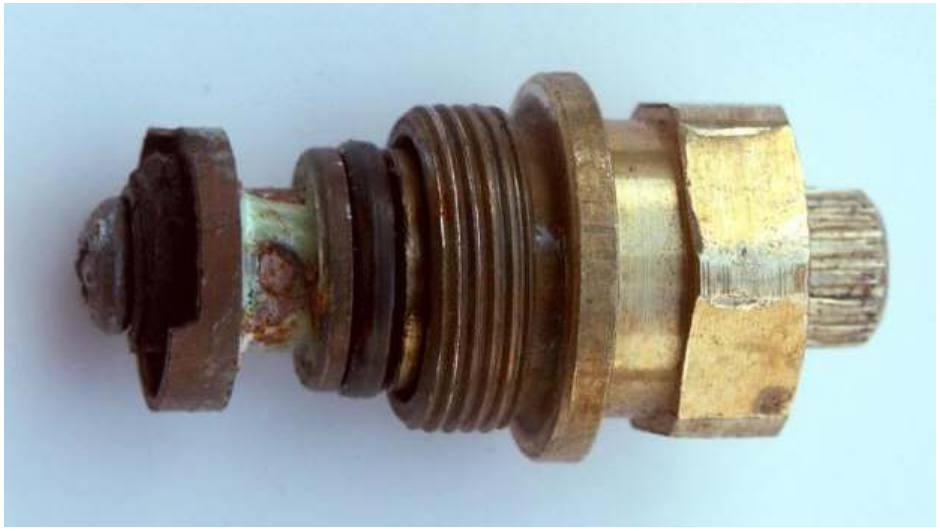

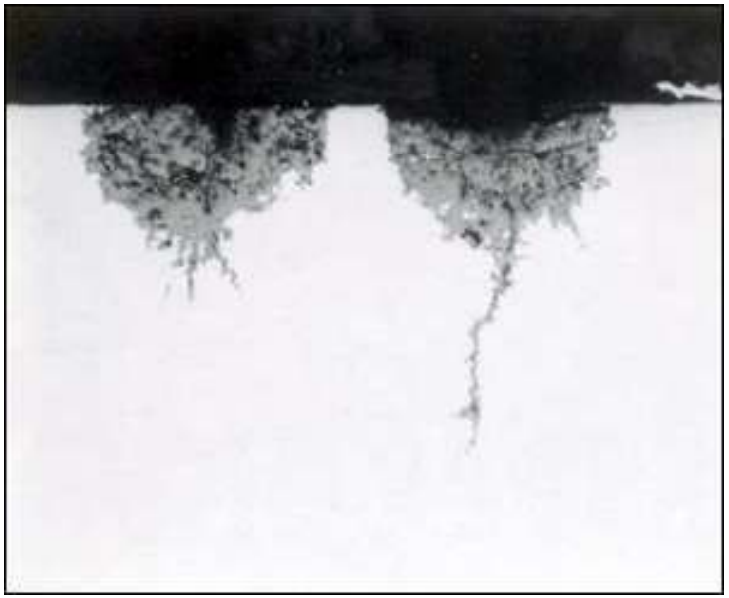

Dezincification plug (100X Original Magnification)

DEZINCIFICATION OF BRASS

It is believed that both copper and zinc gradually dissolved out simultaneously and copper precipitates back from the solution. The material remaining is a copper-rich sponge with poor mechanical properties, and color changed from yellow to red.

Key electrochemical half-reactions generally associated with brass dezincification

Half Reaction	Standard Potential (vs. SHE)	Name	Location
$Zn^0 \rightarrow Zn^{2+} + 2e^-$	0.762V	Zinc Oxidation	Dezincifying Surface
$\frac{1}{2}O_2 + 2e^- + 2H^+ \rightarrow H_2O$	0.814V (pH=7)	Oxidant Reduction	Cathodic Surface
$Cl_2 + 2e^- \rightarrow 2Cl^-$	1.36V		
$Cu^0 \rightarrow Cu^{2+} + 2e^-$	-0.340V	Copper Oxidation	Dezincifying Surface
$Cu^{2+} + 2e^- \rightarrow Cu^0$	0.340V	Copper Deposition	Dezincifying Surface

Wax Actuator submitted for analysis.

Dezincification of brasses is generally limited to alloys that contain less than 85 wt% of copper. Commercial bronze (91 wt% Cu) is considered resistant but not immune to this type of corrosion.

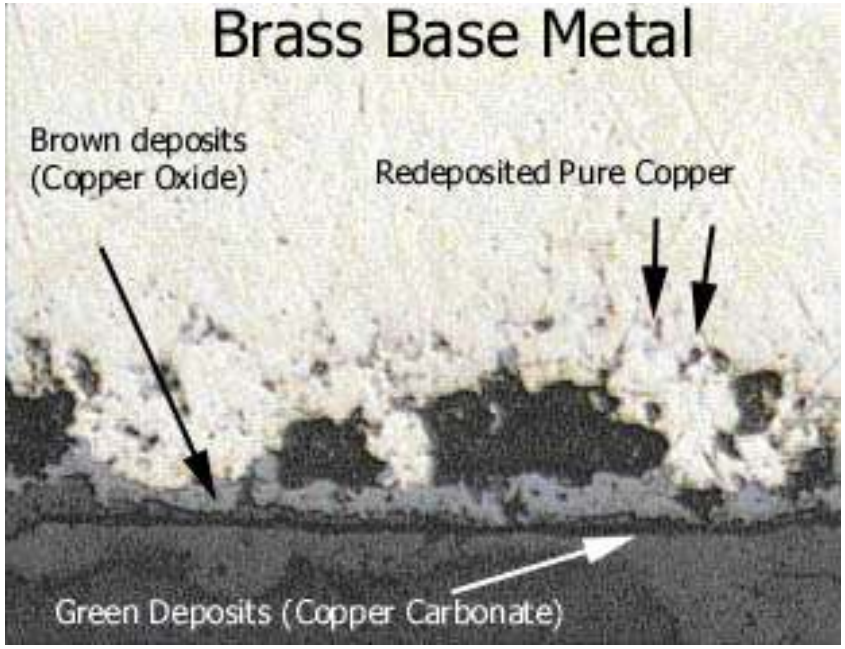

Conditions for dezincification

There are a number of factors that will predispose brass to dezincify:

• Water hardness and the acidity or alkalinity of water away from a pH of 7.
• Temperature. The higher the temperature the greater the risk
• Water flow. Less flow equals greater risk
• Polluted atmosphere
• Large brass grain size
• Sea or brackish water
• Corrosive soils such as acid peat, salt marsh, waterlogged clay, or ‘made up’ ground containing cinders

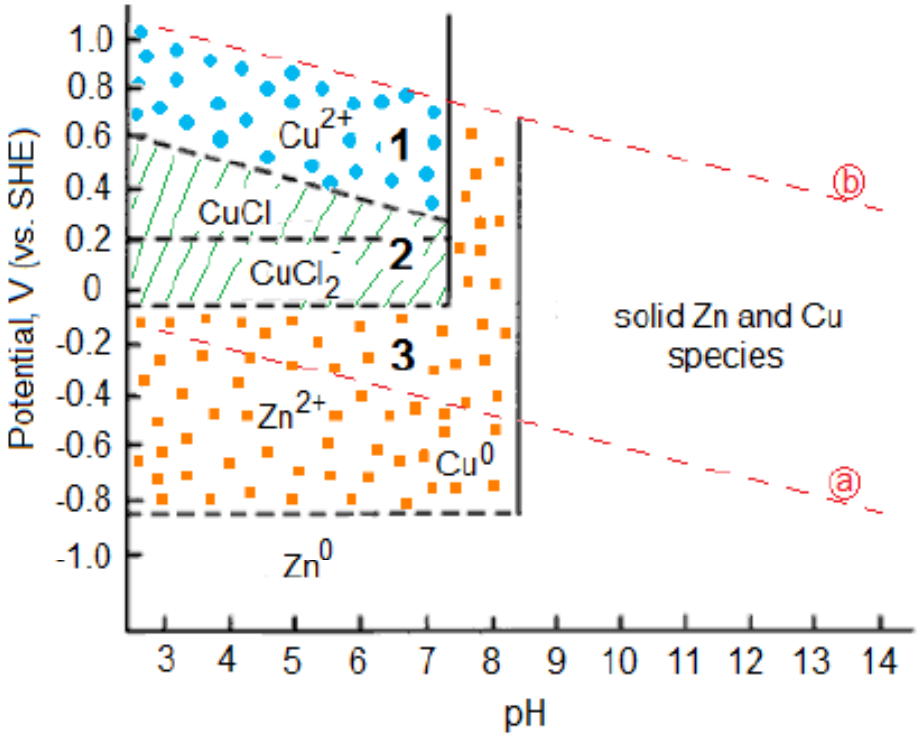

Illustrative potential-pH diagram for 70-30 brass in 0.1M chloride solution (adapted from Heidersbach & Verink 1972/18/). Region 1 represents uniform brass corrosion via copper and zinc dissolution with no copper re-deposition; 2 represents dezincification via copper and zinc dissolution with copper re-deposition; and 3 represents dezincification via selective zinc leaching alone. 2 is particularly relevant to localized environments where chloride concentrations are elevated and pH is reduced. Between lines a and b water is stable. Depending on water chemistry (e.g., chloride concentration) and brass composition, regions will shift

General trends for brass alloys as zinc content is varied.

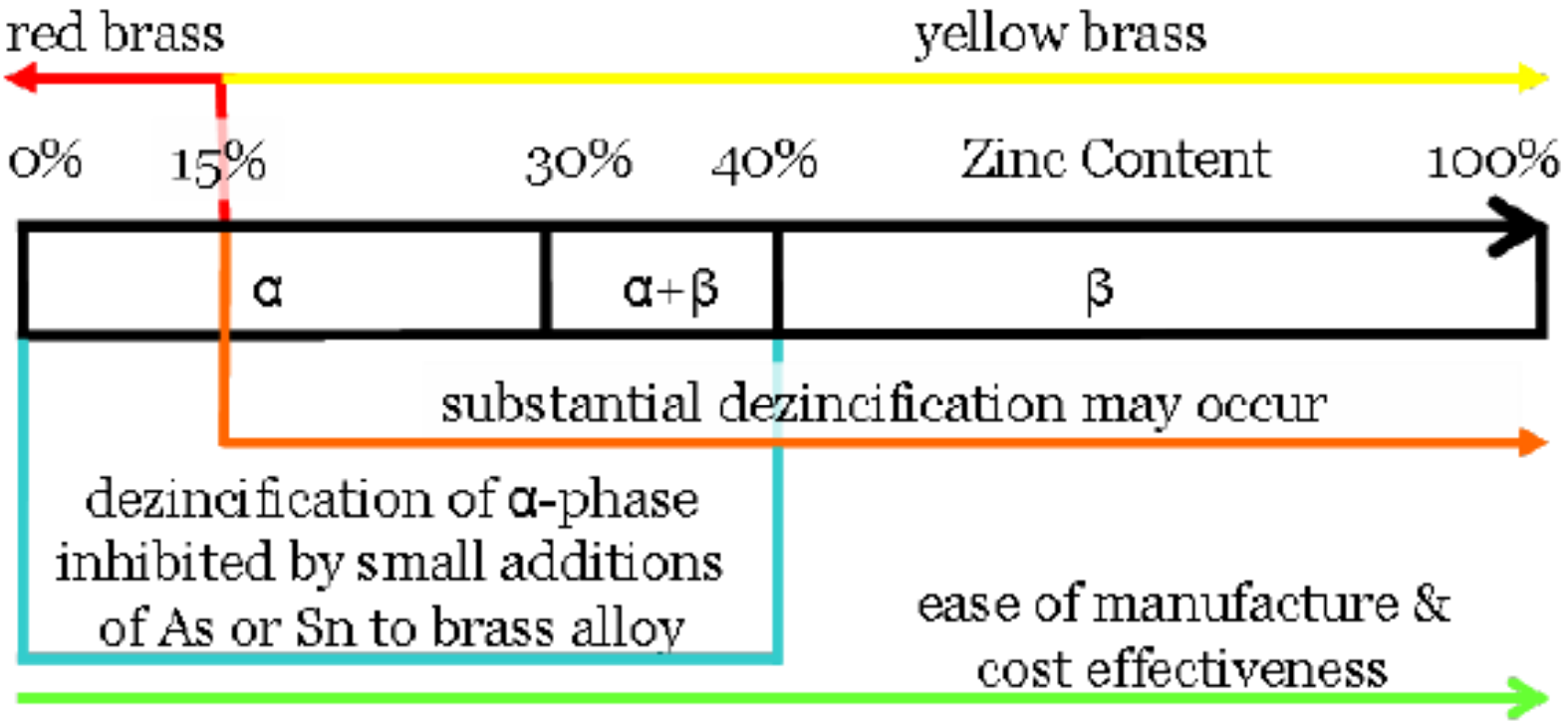

Yaofu Zhang , *Dezincification and Brass Lead Leaching in Premise Plumbing Systems: Effects of Alloy, Physical Conditions and Water Chemistry*, December 9, 2009 ,Blacksburg, Virginia

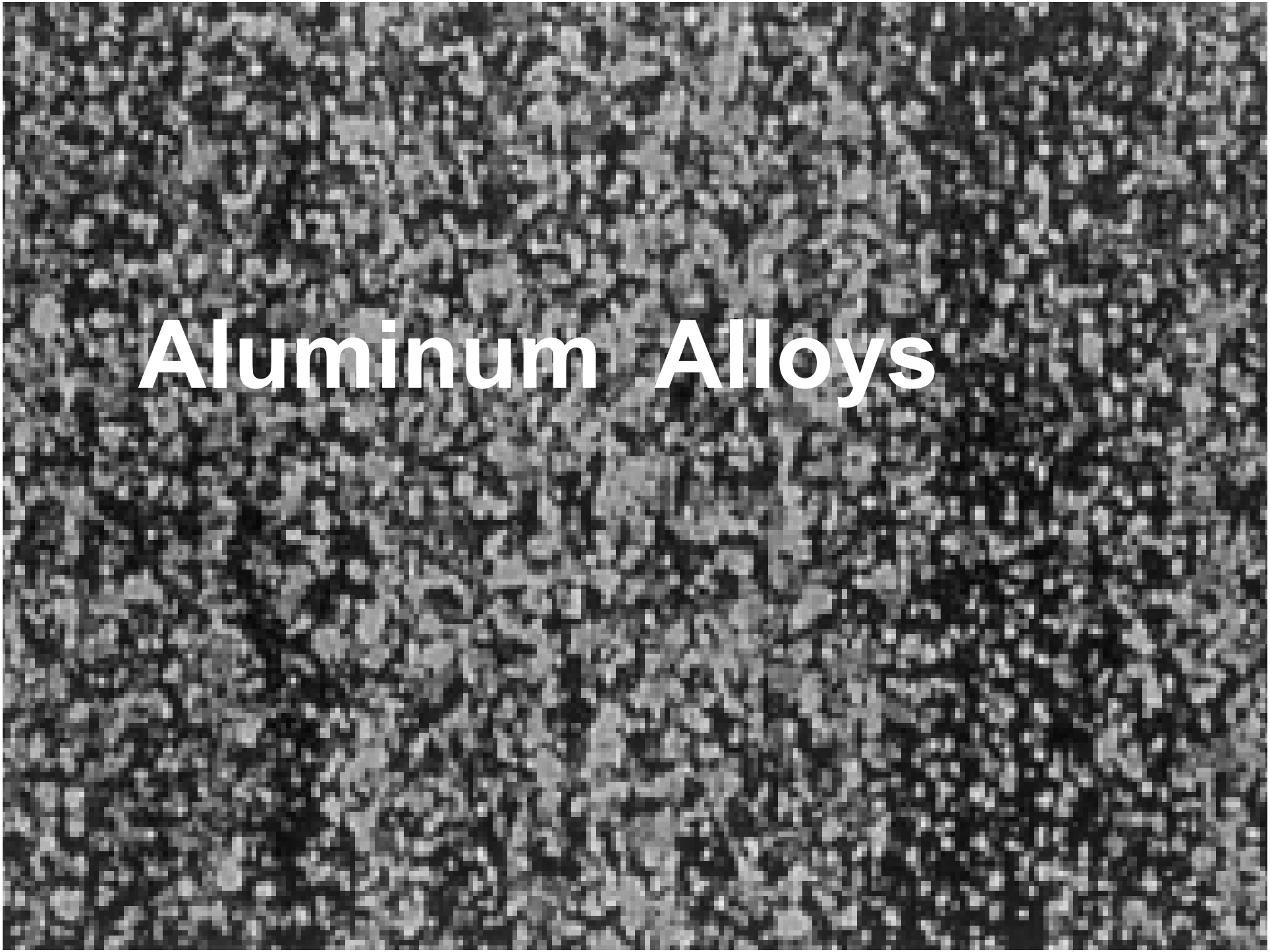
Aluminum Alloys

ALLOY DESIGNATION SYSTEMS

International Alloy Designation System (IADS)

Aluminum alloy designations for wrought alloys

Four-digit series	Al content or main alloying elements
1XXX	99.00% minimum
2XXX	Copper
3XXX	Manganese
4XXX	Silicon
5XXX	Magnesium
6XXX	Magnesium and Silicon
7XXX	Zinc (most also contain Mg)
8XXX	Others e.g. Lithium
9XXX	Unused

Aluminum alloy designations for cast alloys

Three-digit series	Al content or main alloying elements
1XX.0	99.00% minimum
2XX.0	Copper
3XX.0	Silicon, with added Cu and/or Mg
4XX.0	Silicon
5XX.0	Magnesium
6XX.0	Unused
7XX.0	Zinc
8XX.0	Tin
9XX.0	Others

APPLICATION OF MODERN ALUMINUM ALLOYS TO AIRCRAFT

E. A. Starke, Jr. and J. T. Staleyt Proc. Aerospace Sci. Vol. 32, pp. 131-172,1996

The predominate aircraft alloys have been the 2XXX (which includes duralumin, alloy 2017) when damage tolerance is the primary requirement and 7XXX when strength is the primary requirement.

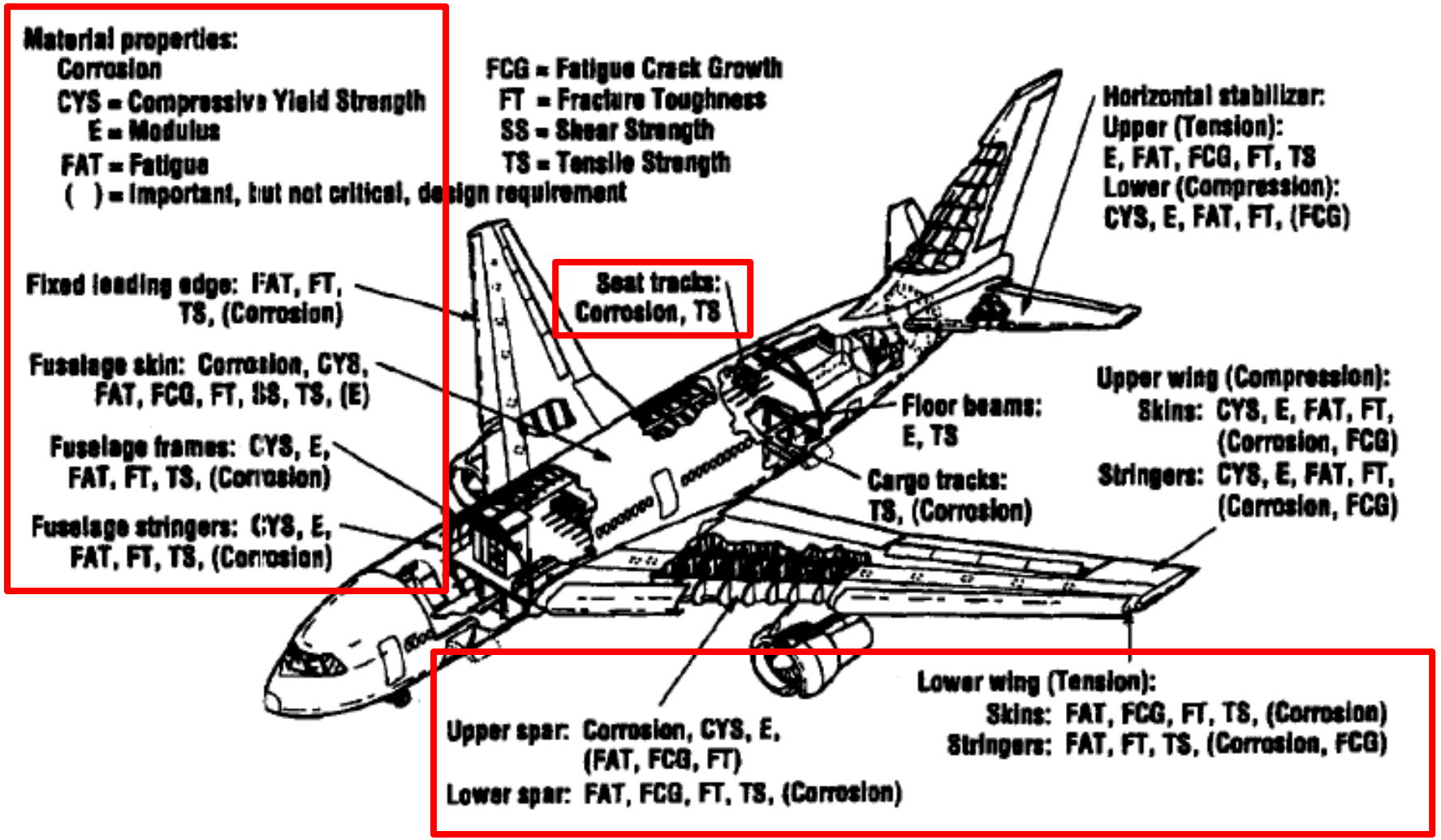

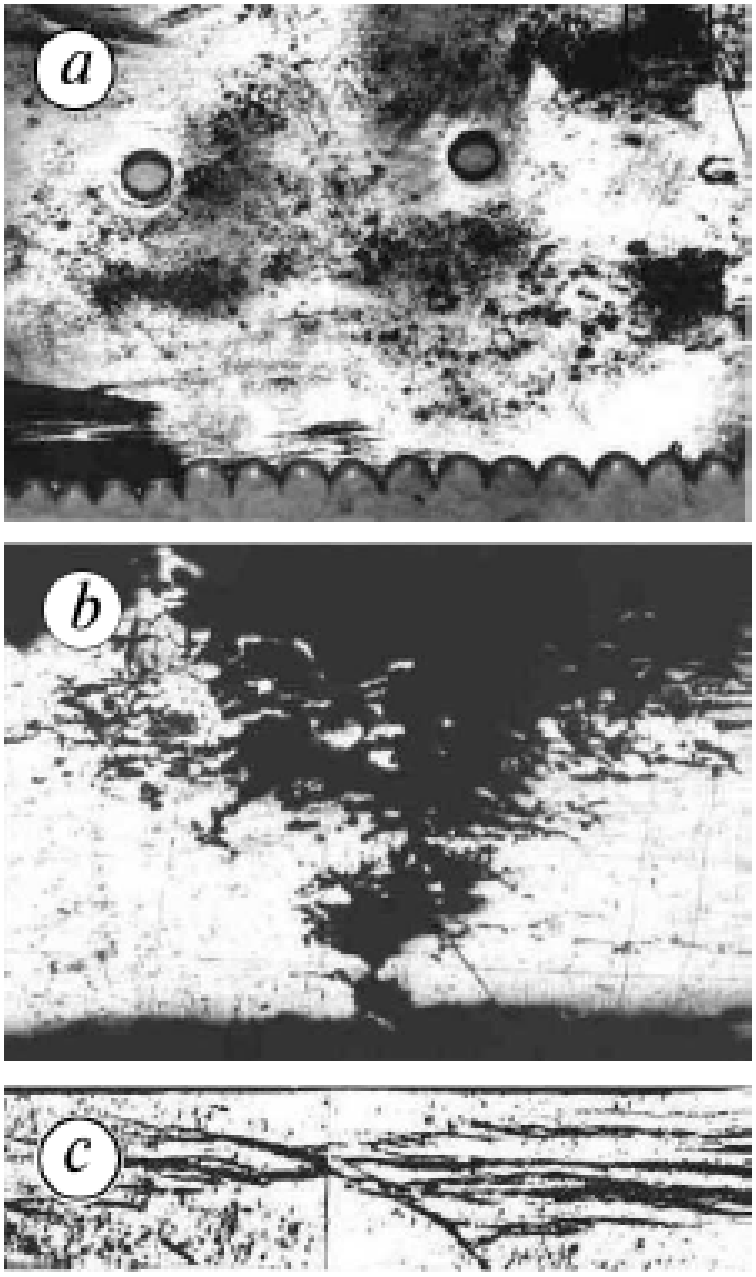

Damages of the fuselage skin by pitting corrosion (× 1.3, a; × 50, b) and of top wing panels by exfoliation corrosion (× 70, c)
after operation of An-24 airplane under conditions of humid tropical climate during 15 and 18 year, respectively.

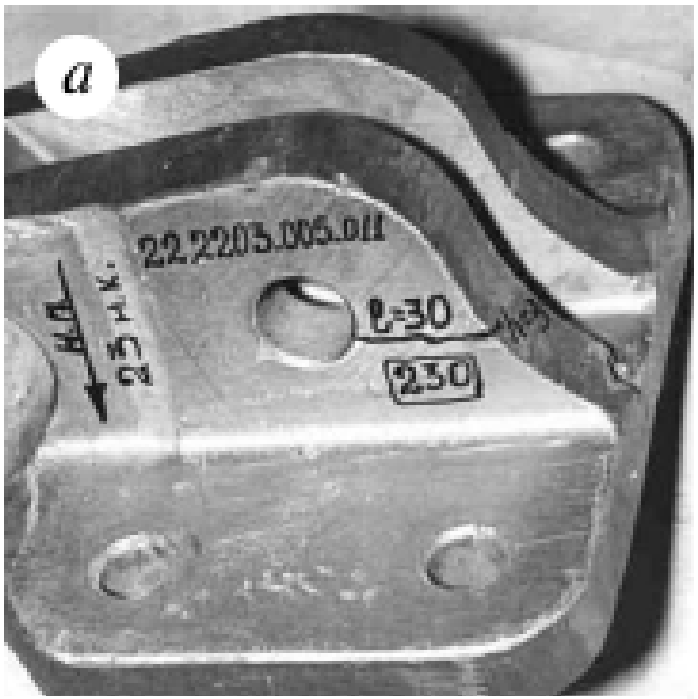

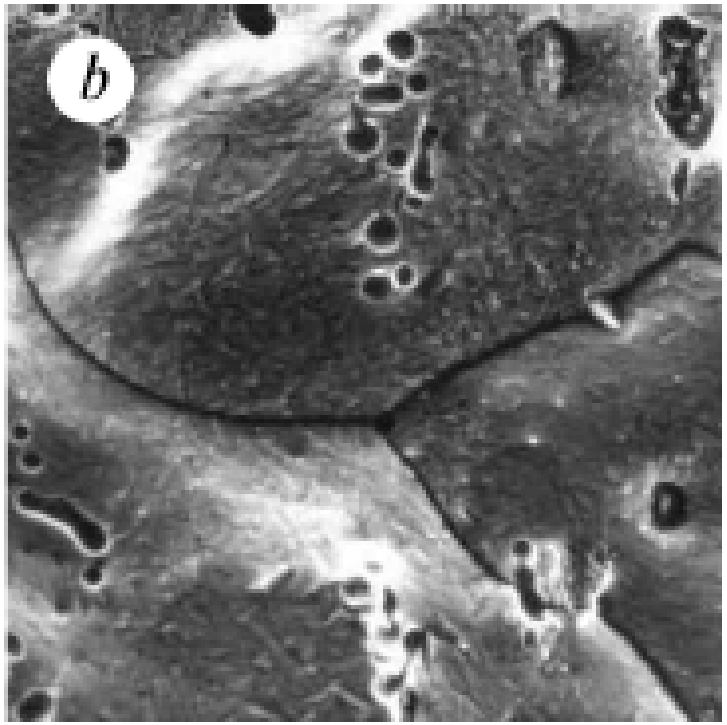

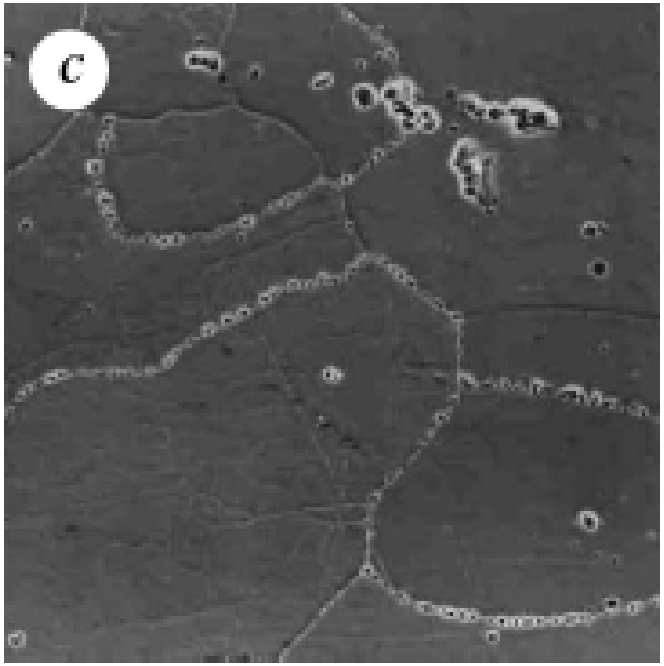

Fracture of the bracket of a flap monorail, made of V93T1 alloy, on An-24 airplane (a), intergranular character of the fracture surface (× 3500, b), and precipitates of the secondary phase along grain boundaries (× 800, c).

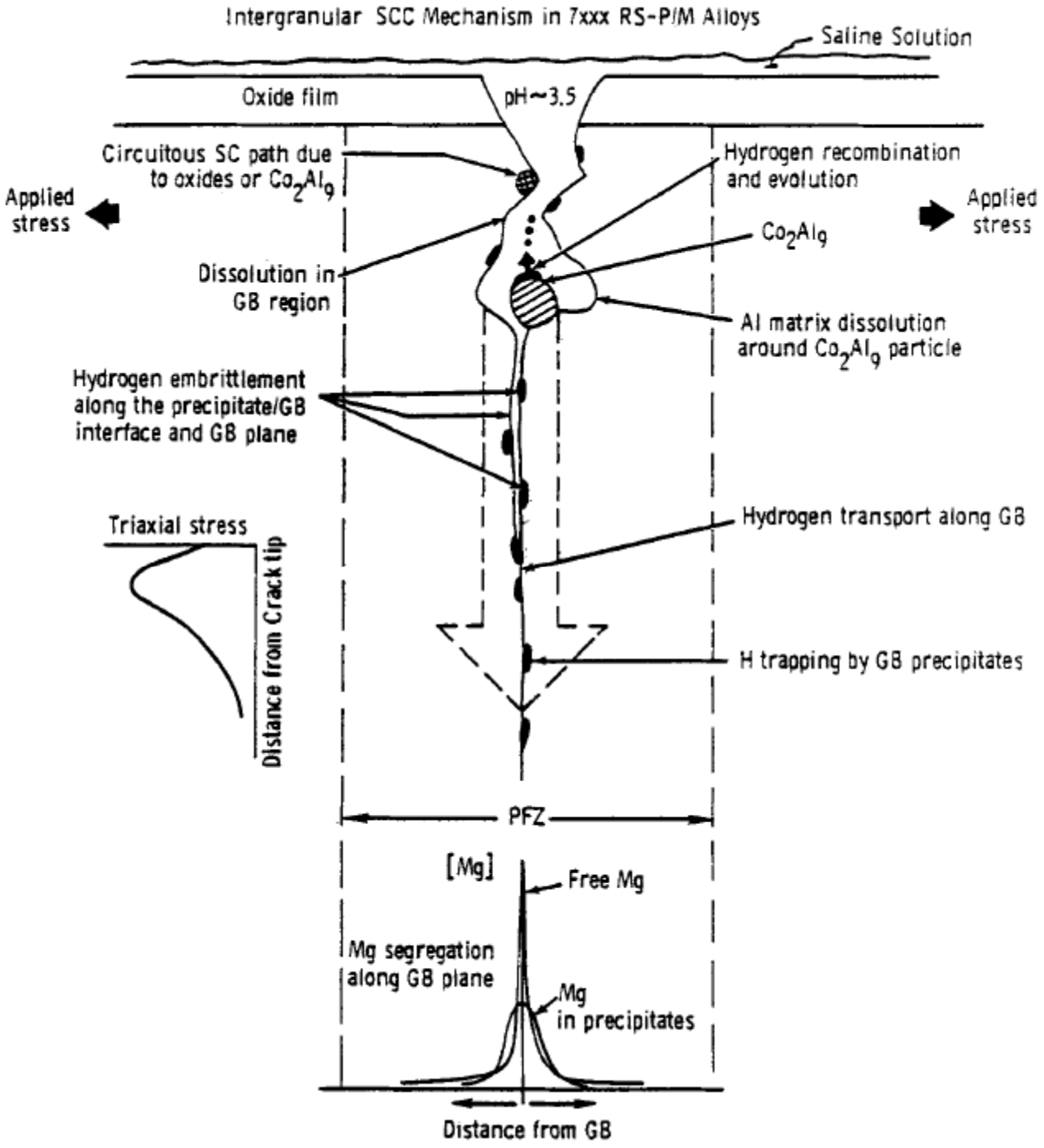
Intergranular SCC Mechanism in 7xxx RS-P/M Alloys
Saline Solution
Oxide film
pH~3.5
Circuitous SC path due to oxides or Co_2Al_9
Applied stress
Hydrogen recombination and evolution
Applied stress
Co_2Al_9
Dissolution in GB region
Al matrix dissolution around Co_2Al_9 particle
Hydrogen embrittlement along the precipitate/GB interface and GB plane
Triaxial stress
Distance from Crack tip
Hydrogen transport along GB
H trapping by GB precipitates
PFZ
[Mg]
Free Mg
Mg segregation along GB plane
Mg in precipitates
Distance from GB

Usual constituents phases in aircraft aluminum alloy products

Alloy	Observed constituent phase(s)
2X24	Al_7Cu_2Fe, $Al_{12}(Fe, Mn)_3Si$, Al_2CuMg, Al_2Cu, $Al_6(Fe, Cu)$
2X19	Al_7Cu_2Fe, $Al_{12}(Fe, Mn)_3Si$, Al_2Cu
6013	$Al_{12}(Fe, Mn)_3Si$
7X75	Al_7Cu_2Fe, $Al_6(Fe, Mn)$, $Al_{12}(Fe, Mn)_3Si$, Mg_2Si
7X50	Al_7Cu_2Fe, Mg_2Si, Al_2CuMg
7055	Al_7Cu_2Fe, Mg_2Si
2090	Al_7Cu_2Fe
2091	Al_7Cu_2Fe, Al_3Fe, $Al_{12}Fe_3Si$
2095	Al_7Cu_2Fe, Al_2CuLi, Al_6CuLi_3
8090	Al_3Fe

Property-microstructure relationships in aluminum alloys

Property	Microstructural feature	Function of feature(s)
Strength	Uniform dispersion of small, hard particles, fine grain size	Inhibit dislocation motion
Ductility and Toughness	No large particles, clean grain boundaries, fine structure, no shearable particles	Encourage plasticity, inhibit void formation and growth, work harden
Fatigue Crack Initiation Resistance	No shearable particles, fine grain size, no surface defects	Prevent strain localization and slip steps on surface, prevent stress concentration
Fatigue Crack Propagation Resistance	Shearable particles, no anodic phases or hydrogen traps, large grain size	Encourage crack closure, branching, deflection and slip reversibility
Pitting	No anodic phases	Prevent preferential dissolution of second phase particles
Stress Corrosion Cracking Hydrogen Embrittlement (HE)	No anodic phases, or interconnected hydrogen traps, hard particles	Prevent crack propagation due to anodic dissolution or HE, homogenize slip
Creep	Thermally stable particles on grain boundaries, large grain size	Inhibit grain boundary sliding

Corrosion of aluminum alloys (atmospheric corrosion)

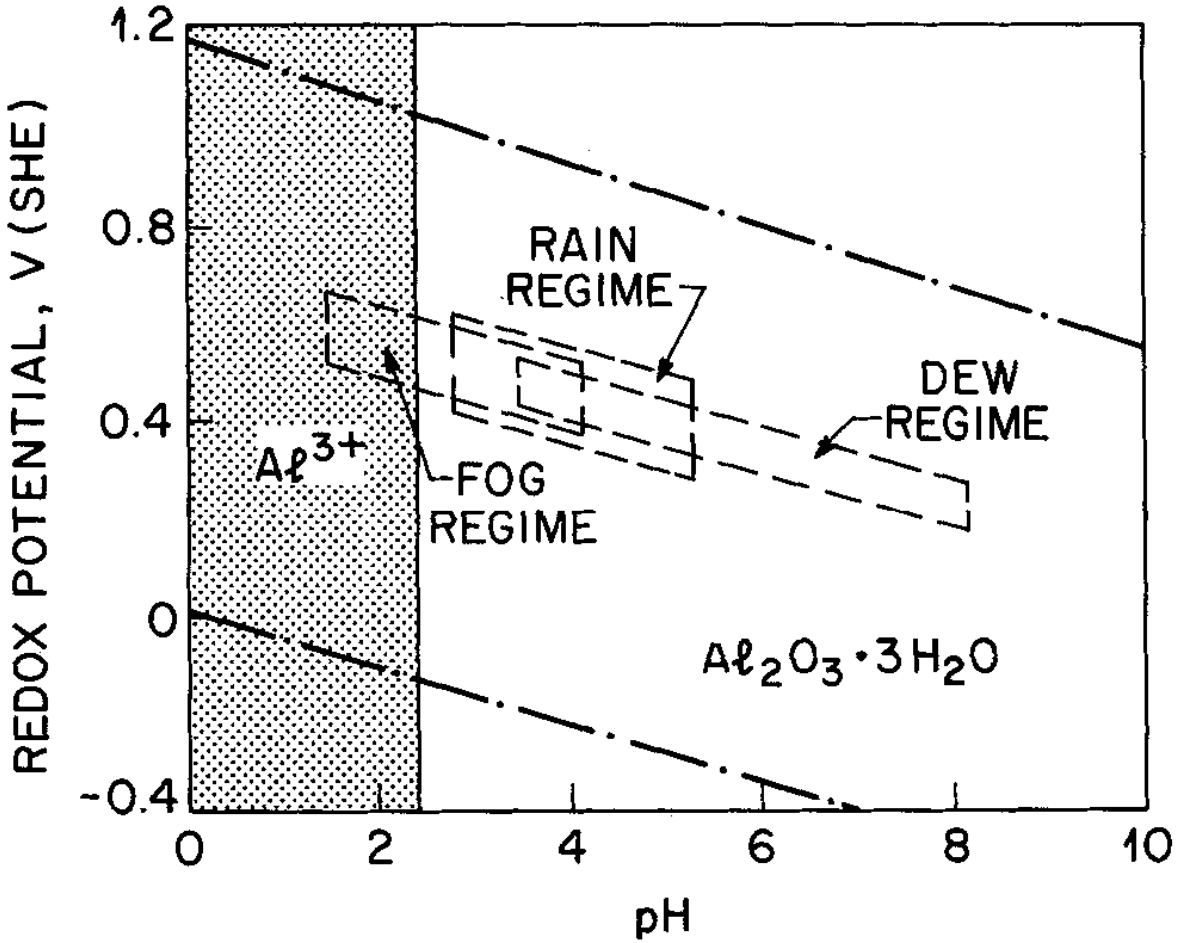

Potential-pH diagram for the system Al-H20 at 25~ for a concentration of aluminum ionic species of 0.1M. The approximate regimes for fog, rain, and dew are indicated

Corrosion of aluminum alloys (atmospheric corrosion)

$SO_2(g) \rightarrow SO_2(aq) + H_2O \rightarrow H^+ + HSO_3^-$

$HSO_3^- + H_2O_2 \rightarrow HSO_4^- + H_2O$

$HSO_3^- + O_3 \rightarrow HSO_4^- + O_2$

$HSO_4^- \leftrightarrow H^+ + SO_4^{2-}$

$xAl^{3+} + ySO_4^{2-} + zOH^- \rightarrow Al_x(SO_4)_y(OH)_z$

Atmosphere polluted by sulfur compounds (acid rain)

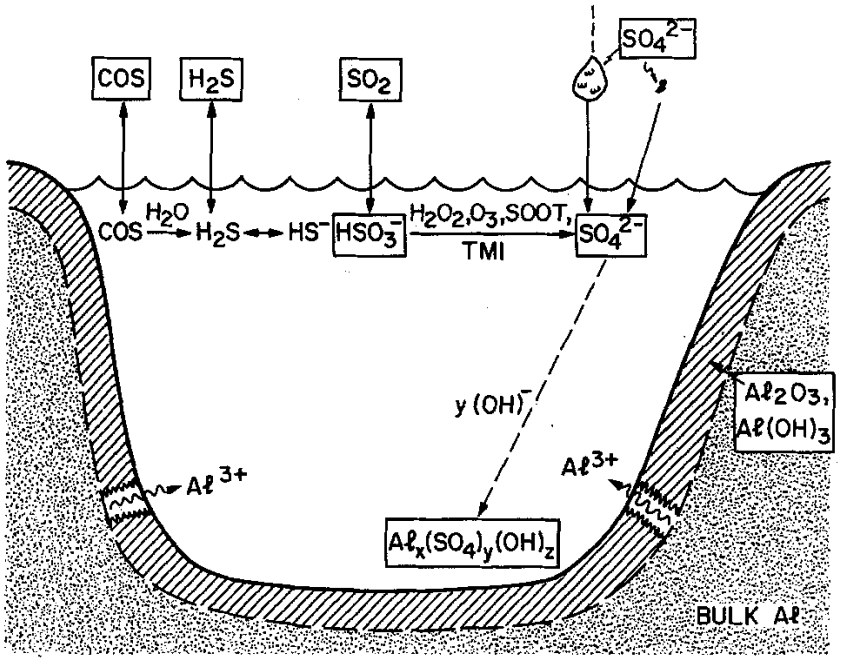

T. E. Graedel, J. Electrochem. Soc., Vol. 136, No. 4, April 1989

Corrosion of aluminum alloys (atmospheric corrosion)

$Al(OH)_3 + Cl^- \rightarrow Al(OH)_2Cl + OH^-$
$Al(OH)_2Cl + Cl^- \rightarrow Al(OH)Cl_2 + OH^-$
$Al(OH)Cl_2 + Cl^- \rightarrow AlCl_3 + OH^-$

$Al + 3HCl \rightarrow AlCl_3 + 3/2H_2$

$AlCl_3 + 3H_2O \rightarrow Al(OH)_3 + 3HCl$

Atmosphere polluted
by chloride compounds

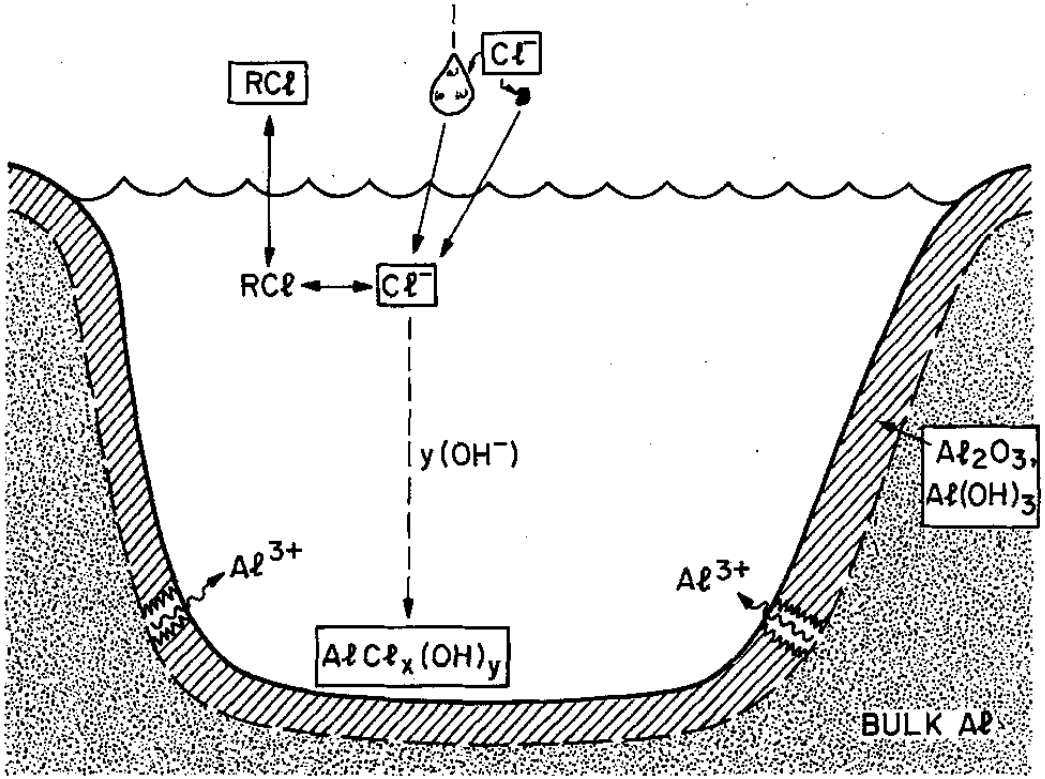

T. E. Graedel, J. Electrochem. Soc., Vol. 136, No. 4, April 1989

Second phase particles in aluminium alloys

Stoichiometry	Phase	Corrosion potential (mV_{SCE}) 0.01 M	0.1 M	0.6 M	Note
Al_3Fe	β	−493	−539	−566	
Al_2Cu	θ	−592	−665	−695	
Al_3Zr	β	−752	−776	−801	
Al_6Mn	-	−839	−779	−913	
Al_3Ti	β	−620	−603	−799	
$Al_{32}Zn_{49}$	T′	−1009	−1004	−1063	
Mg_2Al_3	β	−1124	−1013	−1162	
$MgZn_2$	M, η	−1001	−1029	−1095	
Mg_2Si	β	−1355	−1538	−1536	
Al_7Cu_2Fe	-	−549	−551	−654	
Mg(AlCu)	-	−898	−943	−936	
Al_2CuMg	S	−956	−883	−1061	
$Al_{20}Cu_2Mn_3$	-	−550	−565	−617	
$Al_{12}Mn_3Si$	-	−890	−810	−858	
Al (99.9999)	-	−679	−823	−849	A
Cu (99.9)	-	−177	−232	−220	A
Si (99.9995)	α	−450	−441	−452	A
Mg (99.9)	-	−1601	−1586	−1688	A
Mn (99.9)	-	−1315	−1323	−1318	A
Cr (99.0)	-	−495	−506	−571	A
Zn (99.99)	-	−985	−1000	−1028	A
Al-2%Cu	α	−813	−672	−744	B
Al-4%Cu	α	−750	−602	−642	B
7X75 Matrix	-	−699	−799	−812	M
AA 7075-T651	-	−816	−965	−1180	X

Notes:

A. Pure metal were obtained from Alfa-Aeser and tested using the microcell method.

B. These specimens are homogeneous solid solutions and tested using the microcell method.

M. The phase denoted as 7X75 matrix is the particle-free matrix-phase of AA7474.

X. Tests upon AA7075-T651 were done on bulk specimens using conventional electrochemical methods and an electrode area of 1 cm^2.

Stoichiometry	Phase	Pitting potential (mV_{SCE}) 0.01 M	0.1 M	0.6 M	Note
Al_3Fe	β	442	106	−382	
Al_2Cu	θ	−434	−544	−652	
Al_3Zr	β	−223	−275	−346	
Al_6Mn	-	−485	−755	−778	
Al_3Ti	β	−232	−225	−646	
$Al_{32}Zn_{49}$	T′	-	-	-	C
Mg_2Al_3	β	−818	−846	−959	
$MgZn_2$	M, η	-	-	-	C
Mg_2Si	β	-	-	-	C
Al_7Cu_2Fe	-	−447	−448	−580	
Mg (AlCu)	-	224	−2	-	D, E
Al_2CuMg	S	108	80	135	F
$Al_{20}Cu_2Mn_3$	-	−210	−428	−534	
$Al_{12}Mn_3Si$	-	−563	−621	−712	
Al (99.9999)	-	−545	−610	−696	A
Cu (99.9)	-	19	−30	−94	A
Si (99.9995)	α	-	-	-	A, C
Mg (99.9)	-	−1095	−1391	−1473	A, G
Mn (99.9)	-	-	-	-	A, C
Cr (99.0)	-	479	297	190	A
Zn (99.99)	-	-	-	-	A, C
Al-2%Cu	α	−447	−471	−529	B
Al-4%Cu	α	−418	−406	−465	B
7X75 Matrix	-	−633	−736	−768	M
AA 7075-T651	-	−684	−739	−810	X

Notes:

C. These compounds do not shows a breakdown of passivity, with active dissolution occurring at potentials more positive than E_{corr}.

D. Did not show a breakdown in all cases when tested at 0.1 M NaCl.

E. At the highest concentration of NaCl tested, this compound did not display a breakdown of passivity, with active dissolution occurring at potentials more positive than E_{corr}.

F. The breakdown potential (E_{pit}) of S-phase should be viewed with caution. The electrochemical behavior of this compound is complex[20] and incorporates dealloying of the Al and Mg, capable of generating a relatively large corrosion current density prior to ultimate breakdown. For more details regarding S-phase, see Ref. 20 and 30.

G. The quoted E_{pit} values of pure Mg correspond with the potential at which current density rapidly increases. Pure Mg, however, is generally unstable and freely corrodes in Cl-containing solution.

Second phase particles in Al-Cu alloys

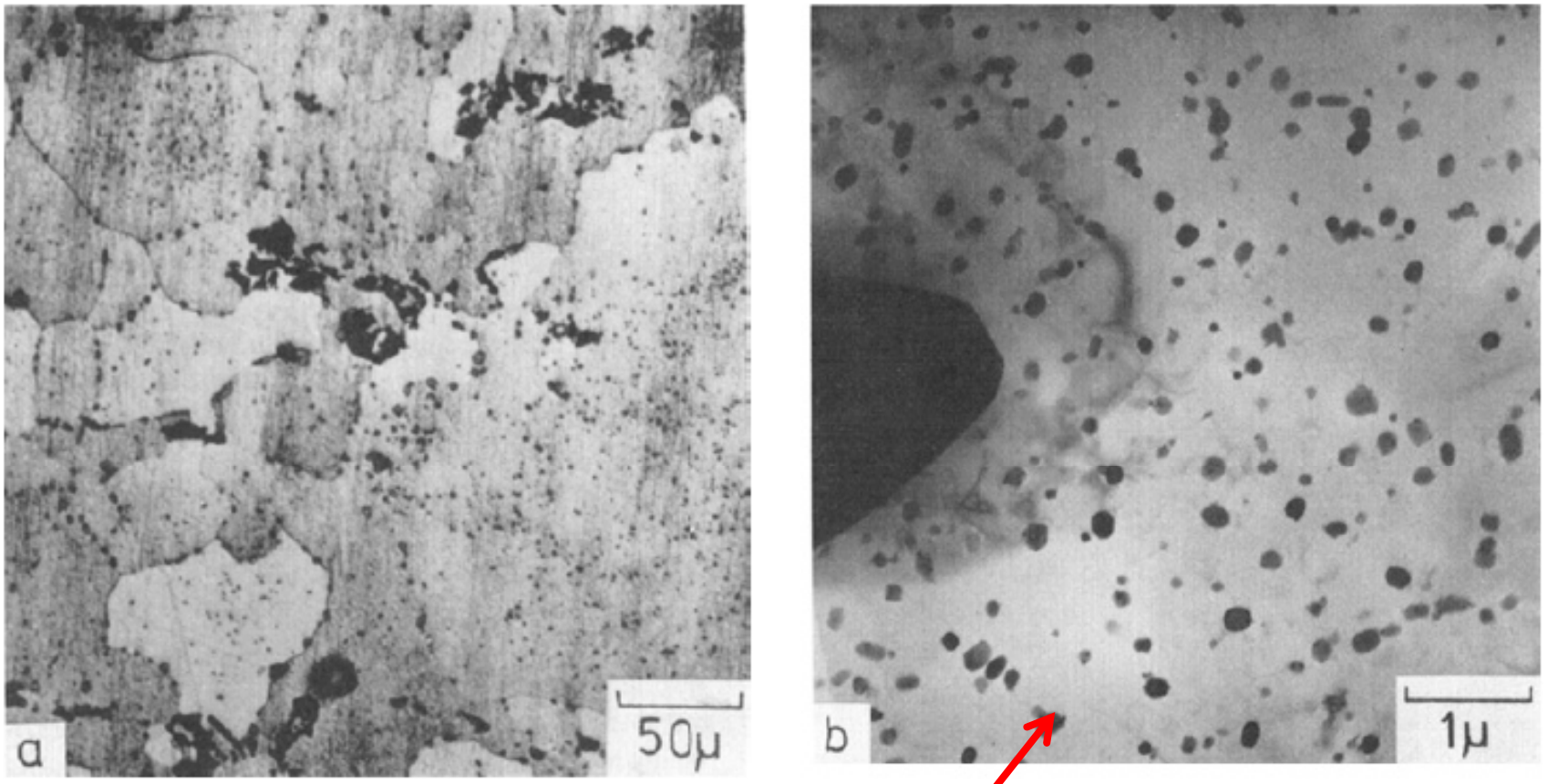

Second-phase particle distribution in the commercial Al-4.3%Cu alloy. (a) Optical micrograph and (b) transmision electrom microscopy image.

Alloy 2014, having a composition: 4.28 %Cu, 0.67 %Mg, 0.72%Mn, 0.83% Si, 0.33% Fe, 0.14% Zn and -<0.05% any other element, balance aluminum.

C-Al(Fe,Mn)Si, $Al_{12}Fe_3Si$ and Mg_2Si intermetallics.

Second phase particles in aluminium alloys

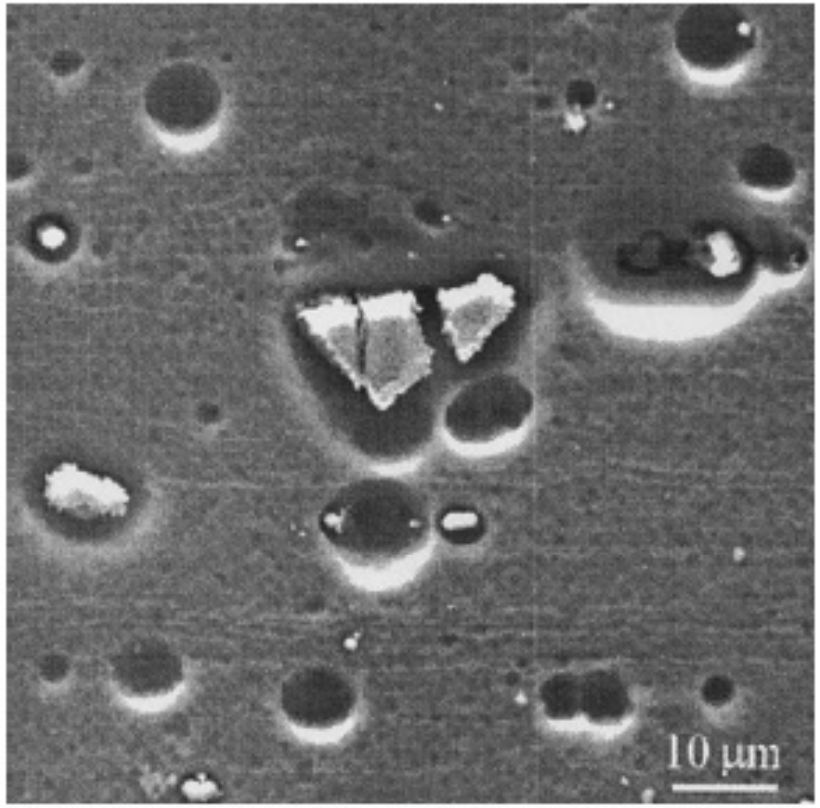

(a)

general pitting

isolated particles

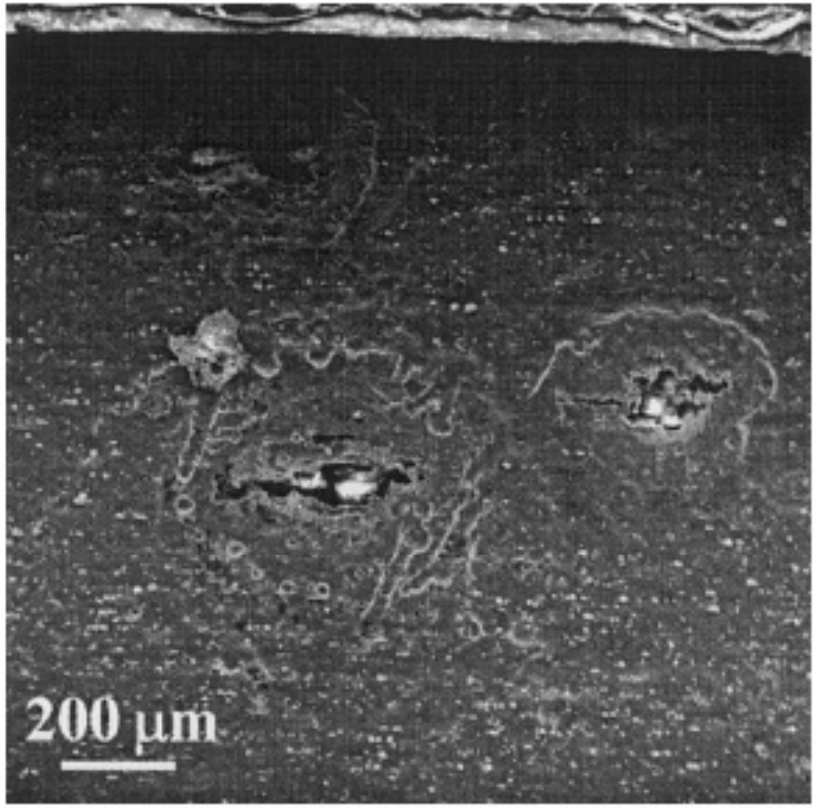

(b)

severe pitting.

particle clusters

Aluminium alloys for the automotive industry

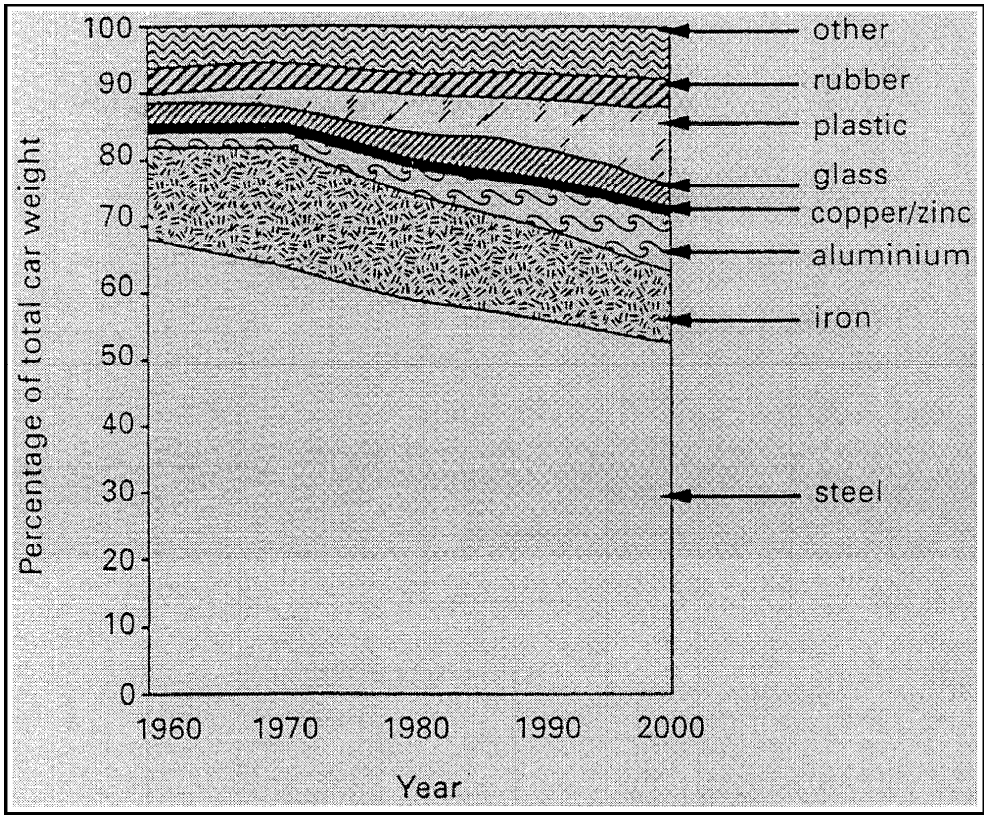

The change in material consumption in average car.

Aluminium castings: engine blocks, pistons, cylinder heads, wheels etc.

Wrought aluminium: heat shields, bumper reinforcements, air bag housings, pneumatic systems, sumps, seat frames, sideimpact panels etc.,

Automotive materials can have an important impact on the environment. The use of lightweight materials can help reduce vehicle weight and improve fuel economy.

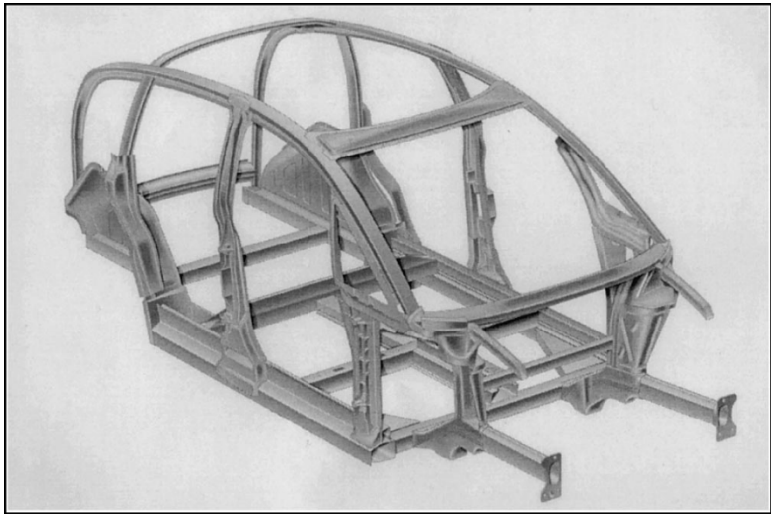

Audi AL2 with an all aluminium body structure.

Aluminium alloys for the automotive industry

Inner panels: 5xxx alloys (Al-Mg)

Outer panels: 6xxx alloys (Al.-Mg-Si)

Aluminium alloys have also found extensive application in heat exchangers.

Aluminium alloys for brazing sheet applications: 6xxx alloys (Al.-Mg-Si-Cu)

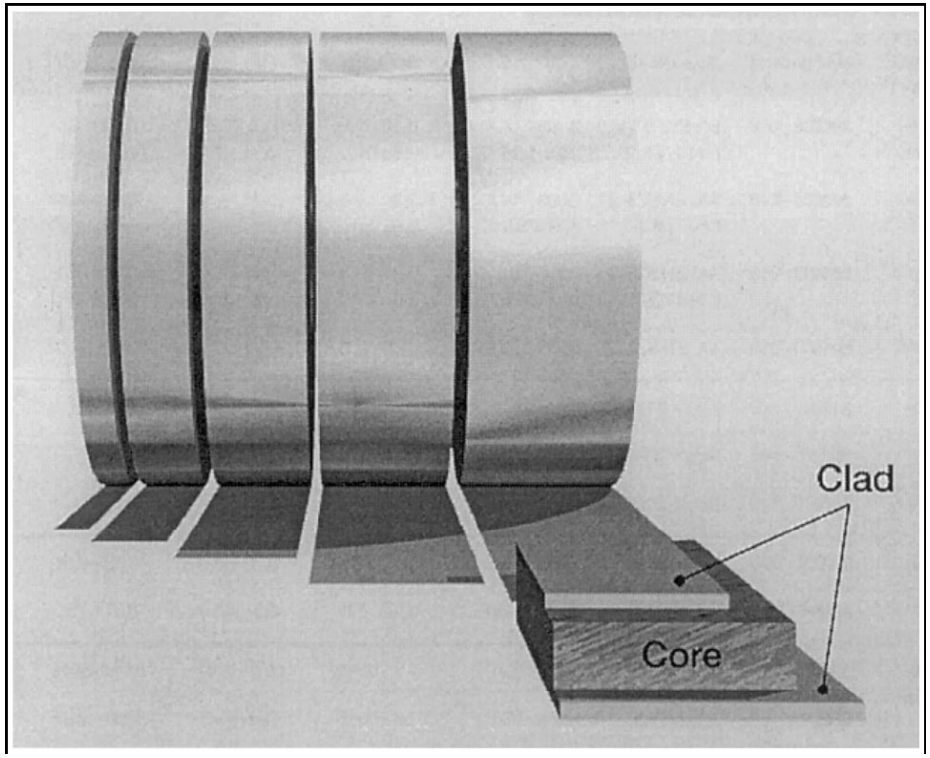

Schematic illustration of a typical brazing sheet.

A sacrificial layer is obtained by Si diffusion from the clad layer into the core. The diffusion stimulates the precipitation of a-AlMnSi particles. This leads to a high density of these precipitates just beneath the clad:core interface, usually called the band of dense precipitates (BDP). This BDP is taking Mn out of solid solution and by this way lowering the corrosion potential of the matrix. Due to the lower corrosion potential of the sacrificial compared to the matrix, corrosion will preferential take place in this layer. This will deflect any corrosion from a pitting mode into a lateral corrosion attack and thus preventing or delaying leakage.

Magnesium Alloys

Corrosion of magnesium

$Mg \rightarrow Mg^{2+} + 2e$ partial anodic reaction

$2H_2O + 2e \rightarrow H_2 + 2OH^-$ partial cathodic reaction

film formation by the chemical precipitation reaction:

$Mg^{2+} + 2OH^- \rightarrow Mg(OH)_2$

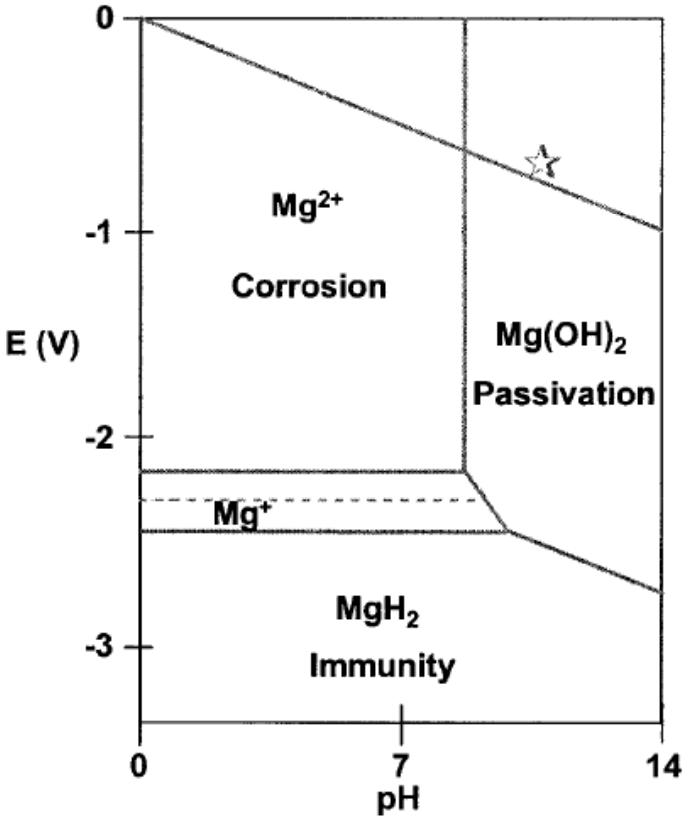

Equilibria of Mg-H_2O at 25 °C

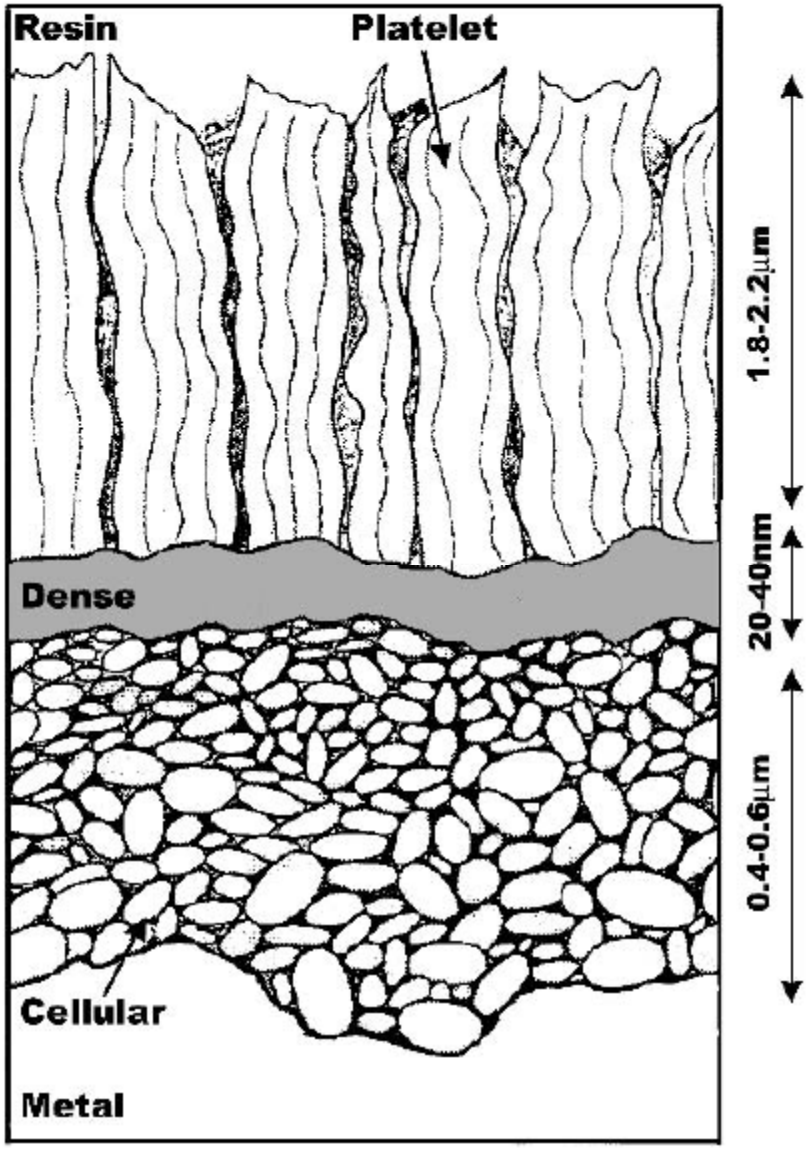

Schematic presentation of the three layer structure of the oxide films on Mg

Results of 2.5 Year Exposure Tests on Sheet Alloys

Material	Corrosion Rate, (μm/year)	Tensile Strength Loss (after 2-5 years, %)
Marine atmosphere		
Al alloy 2024	2.0	2.5
Mg alloy AZ31	18.0	7.4
Low C steel (0.27% C)	150.0	75.4
Industrial atmosphere		
Al alloy 2024	2.0	1.5
Mg alloy AZ31	27.7	11.2
Low C steel (0.27% C)	25.4	11.9
Rural atmosphere		
Al alloy 2024	0.1	0.4
Mg alloy AZ31	13.0	5.9
Low C steel (0.27% C)	15.0	7.5

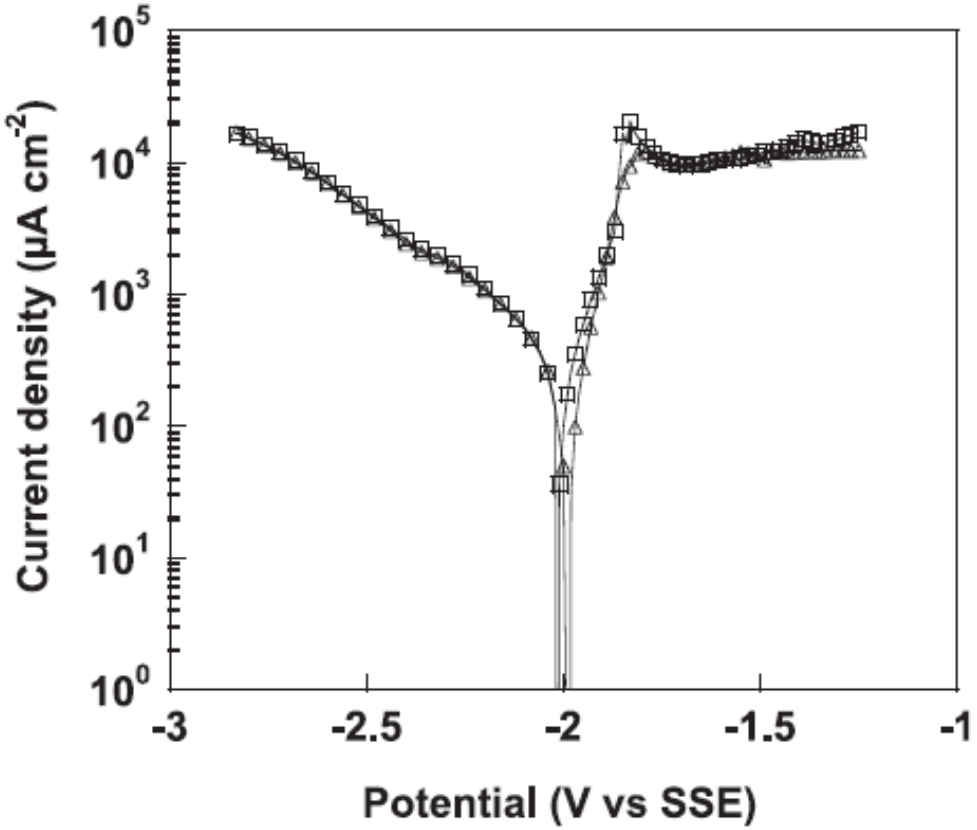

Polarisation curves plotted after a preliminary hold time of 3 h 30 min at Ecorr in 0.1 M Na_2SO_4: 240 rpm; 1000 rpm.

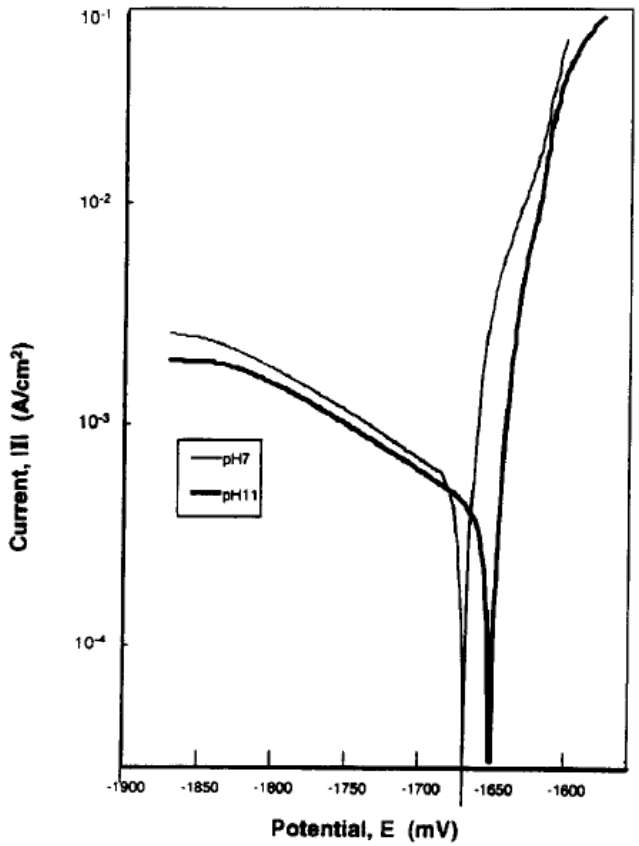

Polarisation curves of magnesium in 1 N NaCl solutions at pH 7 and 11

Schematic presentation of typical possible galvanic corrosion between some of the phases of Mg-Al alloys

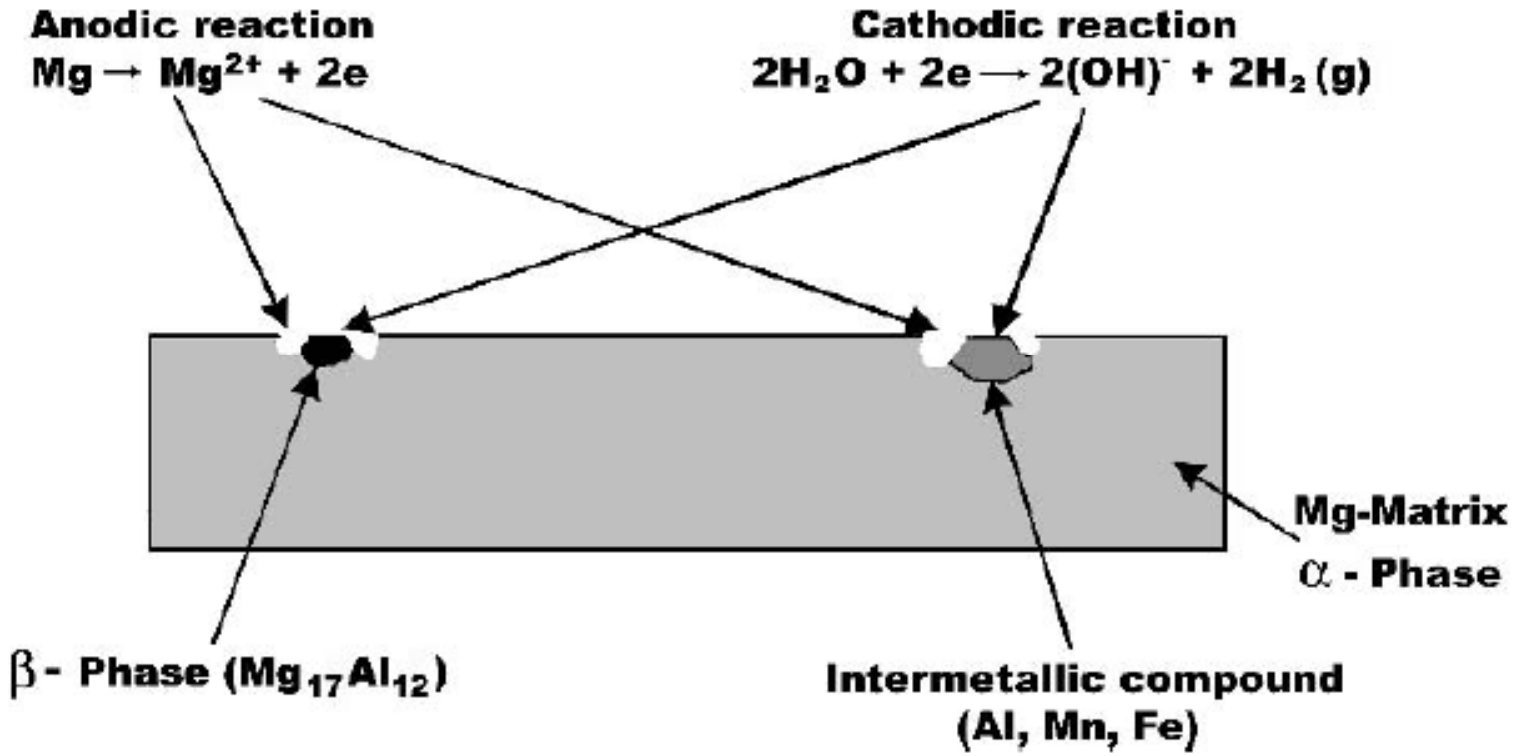

Scheme of pitting corrosion mechanism for magnesium alloy AM60

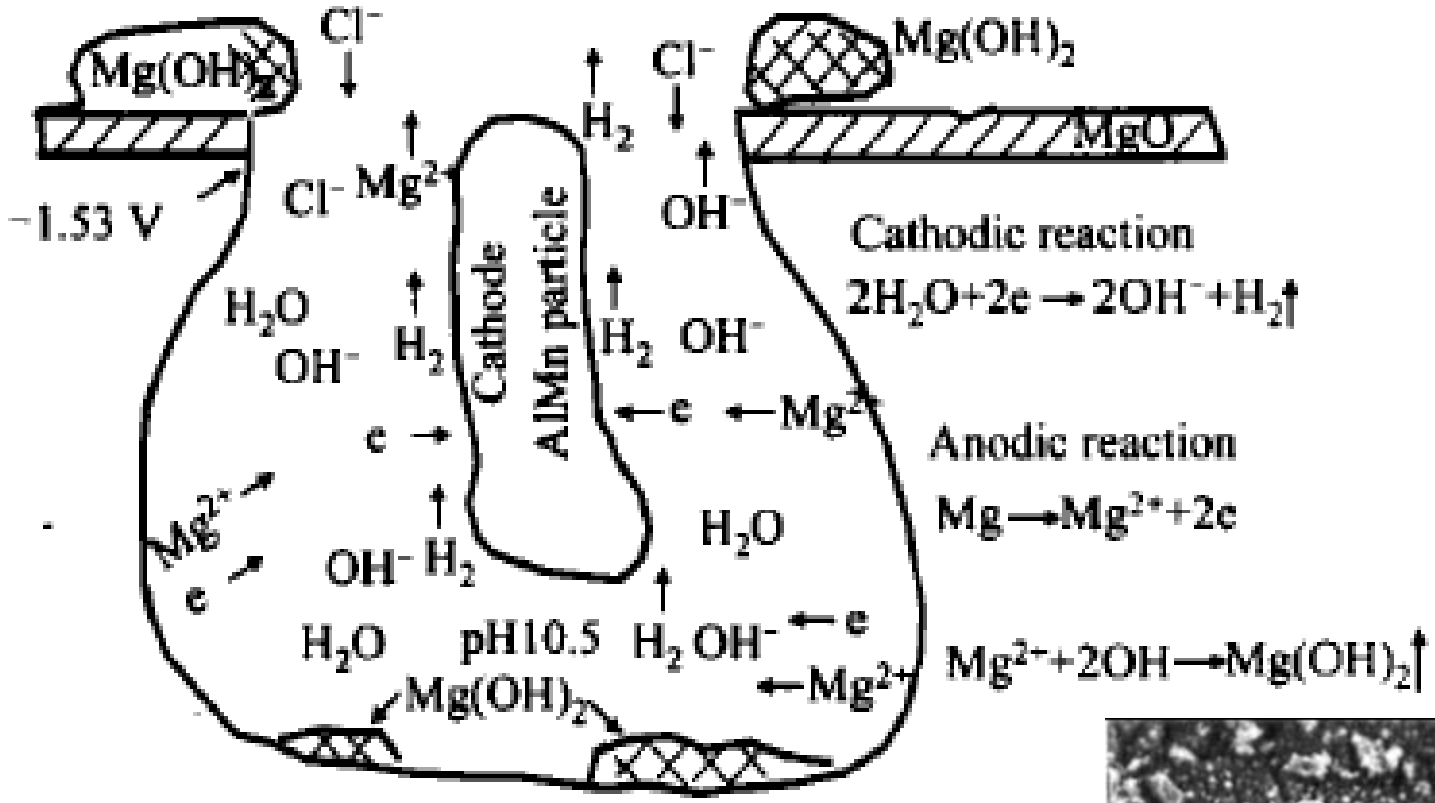

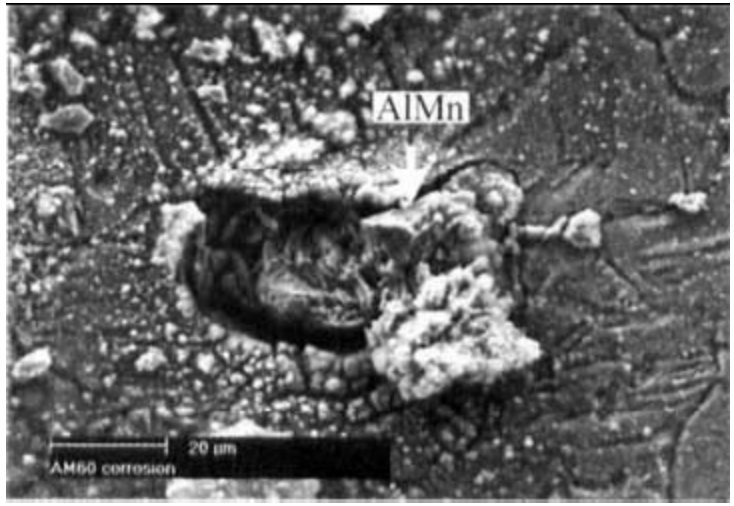

Magnesium alloys

AZ (Mg–Al–Zn) system, containing 2–10% Al with minor additions of Zn and Mn, is the most widely used among Mg–Al alloys. They are characterised by low cost of production and also by relatively good corrosion resistance and satisfactory mechanical properties from 95 to 120 C.

Material	Chemical composition (wt.%)									
	Al	Zn	Mn	Si	Cu	Fe	Ni	Ca	Zr	Others
Mg (99%)	0.006	0.014	0.03	0.019	0.001	0.004	<0.001			
AZ31	3.1	0.73	0.25	0.02	<0.001	0.005	<0.001	<0.01	<0.001	<0.30
AZ80	8.2	0.46	0.13	0.01	<0.001	0.004				<0.30
AZ91D	8.8	0.68	0.30	0.01	<0.001	0.004	<0.008			<0.30

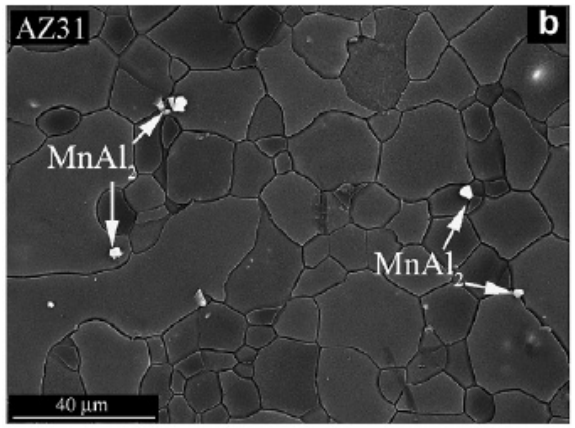

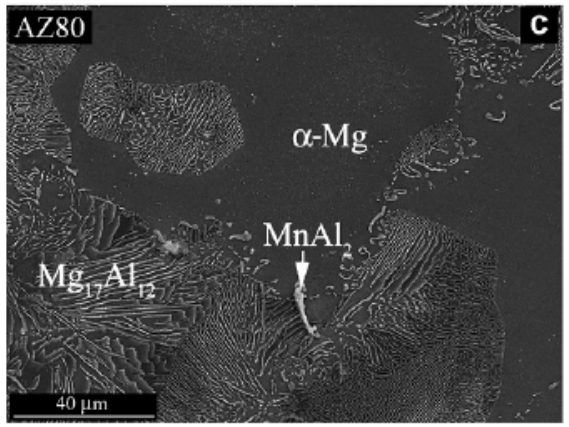

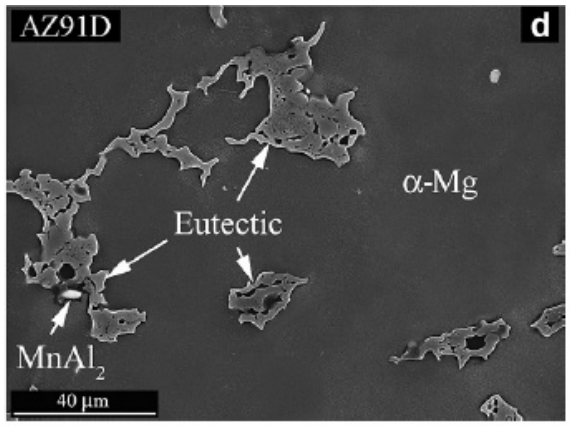

Magnesium alloys

Designation ASTM	Major Alloying Elements	UTS, MPa		Elongation, %		Corrosion Rate, (mg/cm^2/day) (a)	Reference Number
		20 °C	150 °C	20 °C	150 °C		
AZ91D	Commercial (Al, Zn)	260	160	6	18	0.11	3
AE42	Commercial (Al, RE	240	160	12	22	0.12	3
AS21	Commercial (Al, Si)	230	120	16	27	0.34	3
MRI 153M	Experimental Al, Ca, Sr, RE (Be Free)	250	190	6	17	0.09	3
MRI 230D	Experimental (Al, Ca, Sr, RE)	235	205	5	16	0.10	3
AJ62Lx	Experimental (5.6–6.4% Al, 1.7–2.21% Sr)	276		12		0.04	6
AJ62x	Experimental (5.6–6.4% Al, 1.7–2.21% Sr)	240		7		0.11	6
AE	Experimental (5–9% RE)	280		10–12		0.02–0.04 (b)	16
AM60	Commercial (6% Al, 0.13% Mn)					0.055 (b)	16
AXJ	Experimental (0.87–2.6% Ca, up to 0.17% Sr) (c)		(d)		(d)	approx. 0.11	9, 48

(a) 200 h Salt Spray Test (ASTM Standard B-117)
(b) 10 days Salt Spray Test (ASTM Standard B-117)
(c) Optimum overall castability at 2% Ca
(d) 20% greater creep strength than AE42 at 150 °C

Corrosion of magnesium alloys

The addition of aluminium increased notably the corrosion resistance.

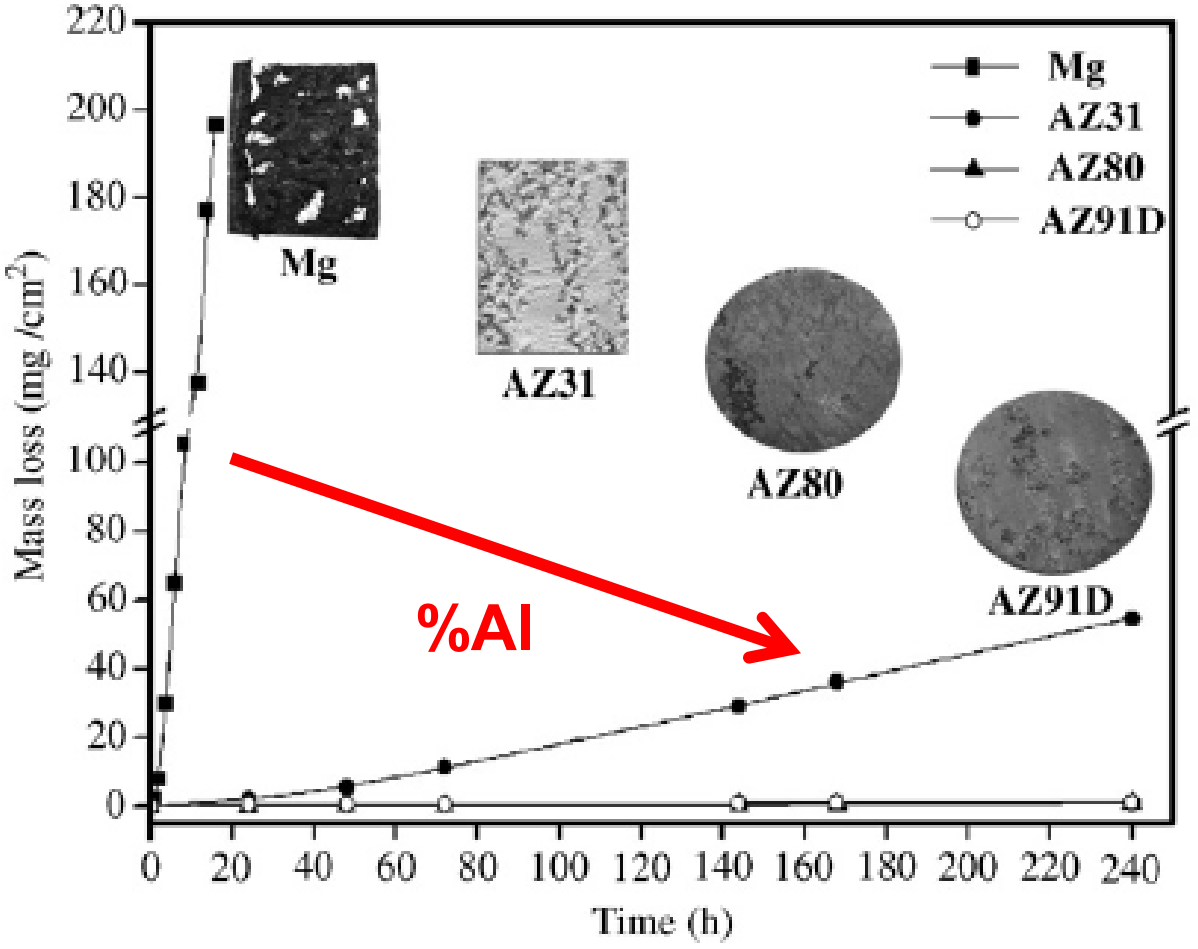

Mass loss versus time for the materials immersed in 3.5 wt.% NaCl solution.

Corrosion of magnesium alloys

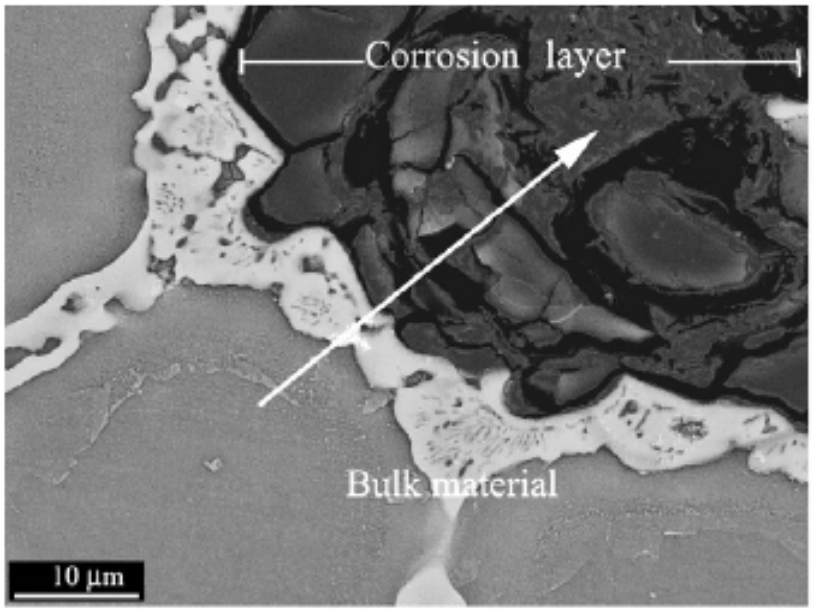

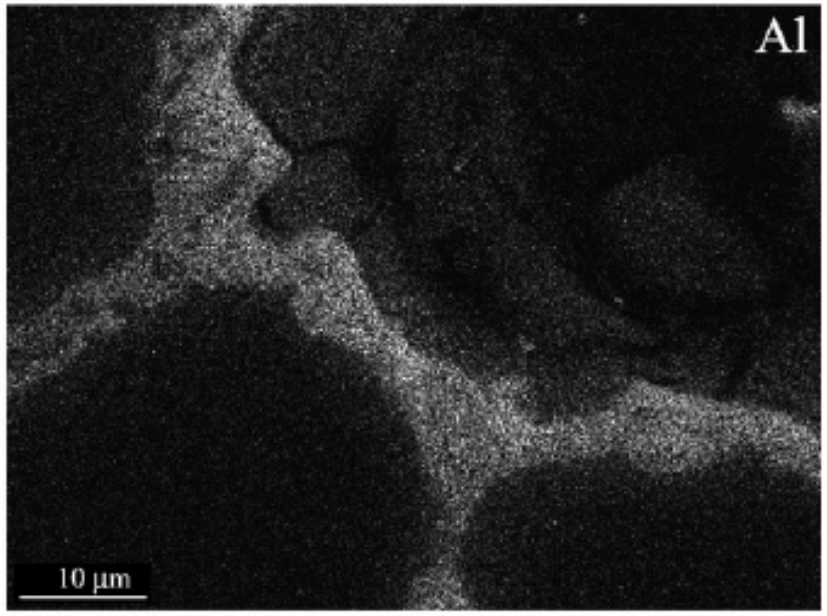

Cross-section BSE image of detail of the corrosion layer, profile line and corresponding X-ray maps of Al for the AZ91D alloy immersed in 3.5 wt.% NaCl for 10 days.

Aluminium enrichment on the metallic surface and allows the formation of a semi-protective Al-rich oxide layer which improves the corrosion resistance of the alloy.

Corrosion of magnesium alloys

Corrosion attack of magnesium alloys occurs at the a-magnesium matrix/Al–Mn and $Mg_{17}Al_{12}$ intermetallic compounds interfaces, by means of the formation of galvanic couples. Later, the nucleation and growth of an irregular and less protective corrosion layer consisted mainly of $Mg(OH)_2$ is produced from α-Mg matrix.

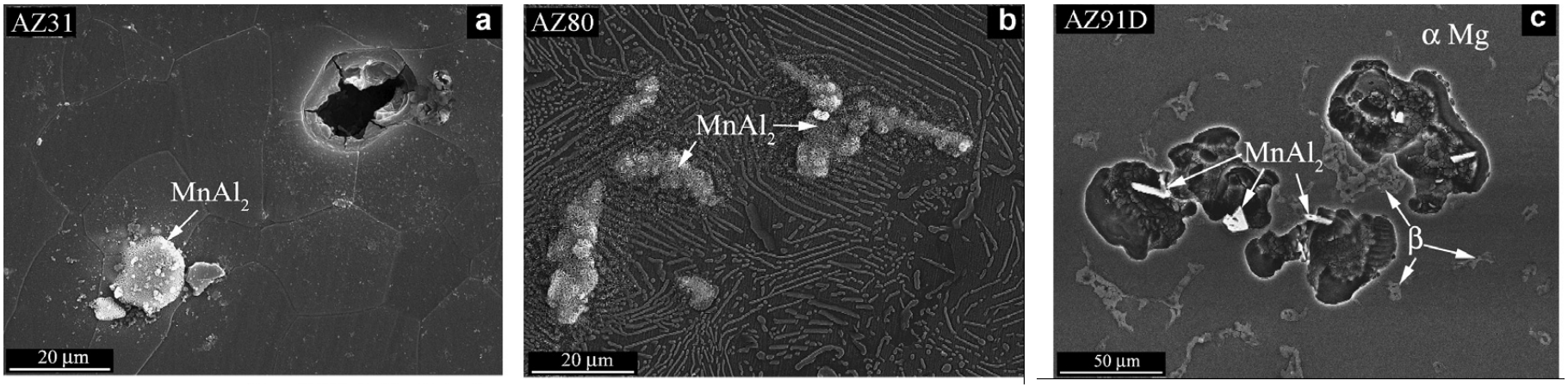

SEM micrographs of alloys immersed in 3.5 wt.% NaCl solution for 2 h: (a) AZ31; (b) AZ80 and (c) AZ91D.

VW Strategy of Magnesium Technology Development

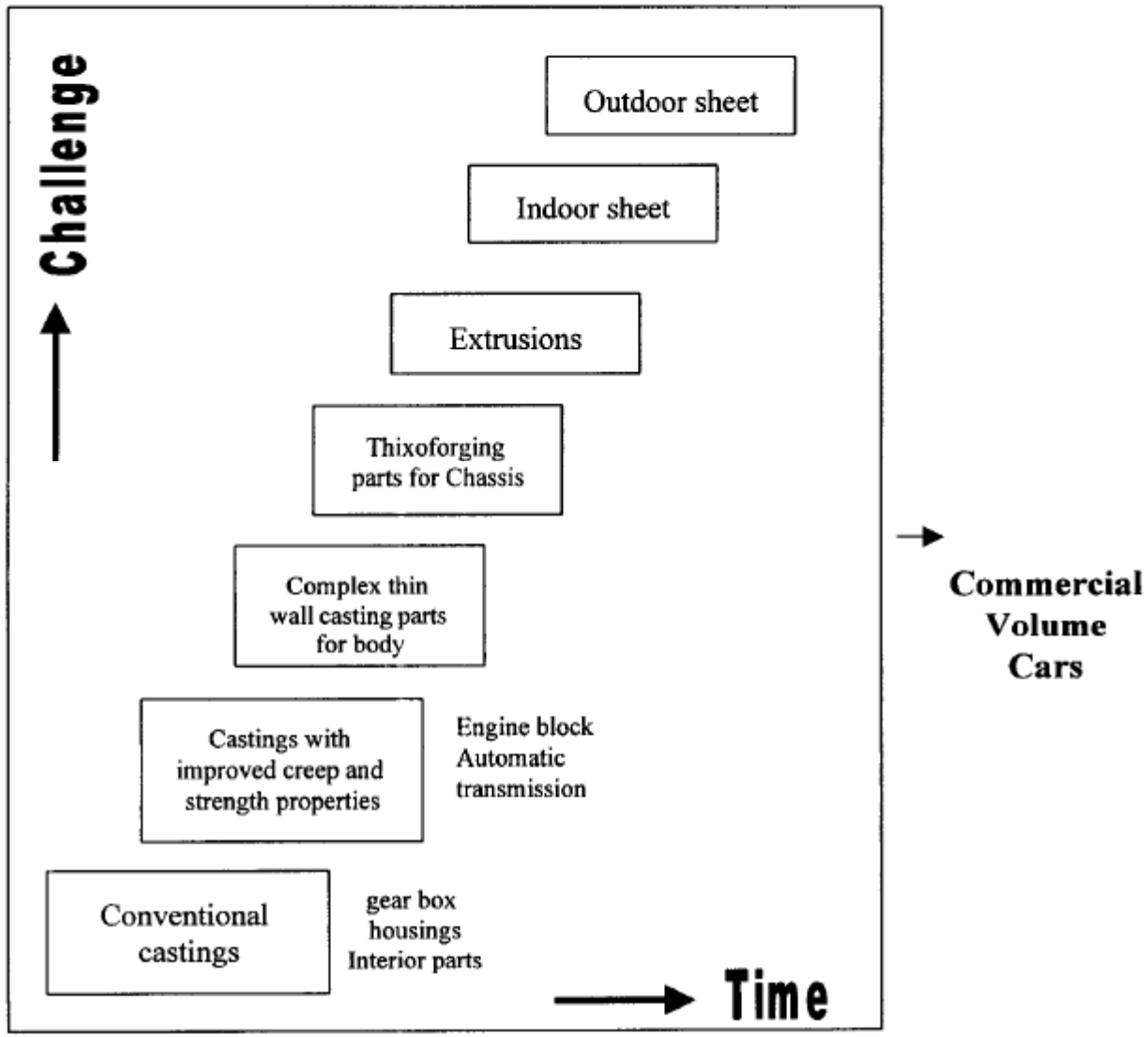

Current and potential application of magnesium alloys in vehicle parts.

Engine and Transmission (drive train) parts	*Interior parts*
Gear box Intake manifold Crankcase Cylinder head cover Oil pump housing Oil sump Transfer case Support	Steering wheel cores Seat components, rear seat Instrument panel Steering column components Brake and clutch pedal brackets Air bag retainer
Chassis components	*Body components*
Road wheels Suspension arms (front and rear) Engine cradle Rear support	Cast components - inner bolt lid section - cast door inner - cast A/B pillars Sheet components Extruded components

Magnesium composite materials

Magnesium matrix composites with **ceramic phases** such as Al_2O_3, TiC, SiC and B_4C as reinforcement have been intensively developed in the past few years because of their high specific strength and stiffness, good wear resistance and low thermal expansion

Intermetallics, similarly to ceramics, are considered to be excellent candidates as reinforcements incomposites since they also have a low density, high strength and a high elastic modulus even at high temperatures. In addition, their thermal expansion coefficients are much closer to those of metals than those of ceramic reinforcements.